DEVELOPMENT OF ADVANCED CATALYSTS FOR WASTEWATER TREATMENT

Moldir Duisengalieva, Bachelor of Chemical Technology of Organic Compounds

Submitted in fulfillment of the requirements
for the degree of Masters of Science
in Chemical Engineering and Materials Science

School of Engineering and Digital Sciences
Department of Chemical Engineering and Materials Science
Nazarbayev University

53 Kabanbay Batyr Avenue,
Astana, Kazakhstan, 010000

Supervisors: Stavros G. Poulopoulos
Vassilis J. Inglezakis

April 2020

Abstract

The presence of emerging pollutants in the water bodies is a relatively new environmental concern. Emerging pollutants involves various chemical substances such as pharmaceuticals, disinfection byproducts, gasoline additives and man-made nanomaterials. The problem is increased inefficiency of conventional treatments in Municipal Wastewater Treatment Facilities (MWTF). In the present work, catalytic and photocatalytic processes were applied to caffeine aqueous solutions. Ag modified zeolites and Fe-doped TiO_2 catalysts were synthesized. Ag modified zeolites were studied using XRD, XRD, TEM, and SEM analysis. The catalytic and photocatalytic efficiency of all catalysts were examined by pH measurements, Total Carbon (TC) analysis and High-performance liquid chromatography (HPLC). Each experiment lasted for 150 minutes and each 30 minutes taken samples were sent to analysis. For Ag modified zeolites ultraviolet light with 254 nm was used, while for Fe – doped TiO_2 catalysts 365 ultraviolet lamp with 365 nm was used. The concentration of caffeine solution was 30 ppm and the volume of the photocatalytic reactor was 500 ml.

The first part of the work was devoted to examine catalytic and photocatalytic efficiency of Ag modified zeolites. The application of ultraviolet light without catalysts achieved 5 % caffeine removal showing the high resistance to ultraviolet light. The overall caffeine removal with all samples of Ag modified zeolites was low (15-20%). In the adsorption process, the highest removal of caffeine was obtained by Ag_2O_NZU catalyst and in the photocatalytic process; it was achieved by Ag^0_NZU catalyst. The study results illustrate the complexity of caffeine structure and the presence of intermediates.

The second part of the work was dedicated to examining the photocatalytic activities of the synthesized Fe-doped TiO_2 catalysts with different iron concentrations (0.5%, 1%, 2%, 4%). The efficiency of photocatalysts were compared with TiO_2 (Degussa P-25) catalyst. The mineralization of caffeine was successfully obtained by using all catalysts. However, TC removal of all catalysts was lower as TiO_2. The obtained results also illustrated the presence of intermediates and not completely degradation of caffeine molecule into carbon dioxide.

Acknowledgements

I would like to express my sincere appreciation to my supervisor Professor Stavros G Poulopoulos for his guidance and support during the research. Also, I would like to thank my co-supervisor, Professor Vassilis J Inglezakis, for all the feedback and encouragement during this research.

Finally, the appreciation extends to Aliya Satayeva for the help of synthesizing Ag modified zeolites in the laboratory and ArdakMakhatova for assistance with TC and HPLC analysis.

Table of Contents

List of Abbreviations & Symbols

TC	Total Carbon
HPLC	High-Performance Liquid Chromatography
UV	Ultraviolet light
SEM	Scanning Electron Microscopy
TEM	Transmission Electron Microscopy
XRD	X-ray powder Diffraction
XRF	X-ray Fluorescence
EDS	Energy Dispersive X-ray Spectrometry
BOD	Biochemical Oxygen Demand
COD	Chemical Oxygen Demand
AOP	Advanced Oxidation Processes
POPs	Persistent Organic Pollutants
PPCPs	Personal Care Products
ppb	Parts per billion
ppm	Parts per million
CTAB	Cetyltrimethyl ammonium bromide
SDBS	Sodium dodecyl benzene sulfonate
OTC	Oxytetracycline
CFA	Coal Fly Ash

List of Figures

List of Tables

Chapter 1 - Introduction

1.1 An overview of Master Thesis

The industrial activities and the world's population growth have significant side effects on the environment. The large amounts of pollutants from domestic, industrial and agricultural applications are being entered into water bodies. These pollutants include several persistent organic pollutants (POPS) such as personal care products (PPCPs), pharmaceuticals, and synthetic dyes. The presence of emerging pollutants has been recognized as significant water pollutants that have adverse effects on both human and wildlife. Nowadays, existing wastewater treatment technologies are not able to easily eliminate this type of pollutants. Therefore, with increasing demand for clean and management of water, developing effective wastewater treatment technologies with high efficiency and low capital requirements are vital. For that purpose, many studies have been done to improve wastewater remediation techniques. As these compounds have great resistance to conventional treatment methods and biodegradation, alternative methods are sought for removing emerging pollutants from water. Searching for convenient technologies to destroy this type of compound technologies such as advanced oxidation and adsorption processes have been assessed as alternative methods for water treatment. Adsorption includes the application of convenient materials to eliminate pollutants from wastewater while advanced oxidation processes are based on the formation of hydroxyl radicals which degrade many refractory organic pollutants with high reaction rates. Although both processes are considered as green technologies for water treatment, these technologies have several limitations. Adsorption is a slow process and requires continuous regeneration of spent adsorbents. On the other hand, advanced oxidation processes need expensive chemicals. Integration of several water treatment processes can enhance the general performance of the process and in certain cases can reduce treatment costs. Therefore, the combination of adsorption and advanced oxidation process can improve treatment efficiency and reduce energy/chemical requirements.

1.2 Aims & Objectives

The main objective of the thesis is to study catalytic and photocatalytic processes to treat wastewaters containing emerging pollutants. The research was done in two directions in order to develop photocatalytic materials: a) preparation of silver doped zeolite materials

for the treatment of wastewaters under UV light, b) preparation of Fe-doped TiO_2 catalysts under UV light. The overall total carbon present will be identified by the percentage of total carbon removal. The effectiveness of performed experiments will be defined by the caffeine concentration in the presented samples. The characterization of materials can be tested by using several types of advanced techniques. The first part will be devoted to obtain modified zeolites consisting of clinoptilolite. The second part will be dedicated to synthesizing Fe-doped TiO_2 catalysts with different concentrations and study their photocatalytic efficiency.

1.3 Thesis structure

The current master thesis consists of 5 chapters. The first section is the introduction. This chapter is emphasized the general information about the research problem, presenting the aims and objectives of the thesis, and showing the structure of the master thesis.

The second section is devoted to the literature review. This section gives information about conventional wastewater treatment technologies and the current research in Advanced Oxidation Processes. Furthermore, it presents the application of natural and synthetic zeolites for the removal of different emerging pollutants and the application of the Fenton process, current study results in these areas.

The third section is dedicated to the describing methodology of performed experiments. This chapter presents the synthesis of Ag modified zeolites, synthesis of Fe-doped TiO_2 catalysts. Furthermore, it contains a reactor configuration and how experiments were performed.

The fourth section emphasizes the results and their discussion. There are primarily two sets of experiments were performed. The first one of the tests that were done with Ag modified zeolites. The second one was performed by using Fe-doped TiO_2 catalysts. The results of the experiments were analyzed by Total Carbon (TC) and High Performance Liquid Chromatography (HPLC).

Finally, the last chapter is devoted to the outcome of the work presented in this thesis. The future work and possible recommendations are mentioned in this section.

Chapter 2 –Literature review

2.1. Emerging pollutants in water

Each year the large amounts of pollutants from domestic, industrial and agricultural applications are being entered into the environment. According to this, water contamination has become endangering for both humans and ecosystems. These issues have been spread to the world and also constrained economic growth in certain aspects [1]. Water quality studies generally give attention to metals, nutrients, microbial pollutants, and priority pollutants. However, in recent years research reveals the existence of organic pollutants which considerably affect the water quality. These pollutants derive from a variety of sources and usually exist in concentrations from ng L^{-1} to µg L^{-1} [2]. This group of contaminants termed as emerging contaminants that relate to new contaminants in water or new impacts and features of organic substances which already exist in the environment [3]. Emerging pollutants are synthetically and naturally occurring substances that are not regulated in environmental monitoring programs, but also might be a candidate for future regulations due to its detrimental effects and persistence. This group of pollutants includes a large variety of chemical compounds such as pesticides, pharmaceuticals, and personal care products and hormones that have crucial adverse effects for both humans and wildlife [4]. As reported by Houtman [5], emerging pollutants are divided into three categories. The first category contains compounds that are recently established in the environment, namely industrial compounds. One of the newest groups of emerging pollutants are artificial sweeteners. These substances are used in large volumes as sugar alternatives. Examples are saccharin, cyclamate, sesulfame, sucralose. The second category involves compounds that have been presented in the environment for a considerable time but have only been currently discovered. The presence of various types of pharmaceuticals such as bezafibrate metaprolol, carbamazepin, amidotrizoic acid, and sulfamethoxazole were observed in surface waters.

The third category includes compounds that are probably identified for a long period, but just currently detected possible adverse human health and ecological effect. Examples are organophosphate flame retardants, with tris(2-chloroethyl)phosphate and tributylphosphate.

The above seven hundred emerging pollutants are classified in twenty classes. The prominent classes are pesticides, disinfection by-products, pharmaceuticals, industrial chemicals, and wood preservation. Emerging pollutants are not controlled by international routine monitoring programs and their toxicological effects, fate and behavior are poorly understood [6].

However, Rodil et al. [7] claimed that the conversion of emerging pollutants by the drinking water technology process may produce substances that can be more persistent, toxic and less biodegradable than their parent compounds. Guillen et al. [8] illustrated the crucial adverse effects of emerging pollutants such as bioaccumulation, toxicity, persistence, biomagnifications, endocrine disruption potential, mutagenic and teratogenic effects. Fawell and Ong [9] determined that some emerging pollutants may be detrimental for both aquatic organisms and humans, with foetal malformation, endocrine disturbing effects, hormone disruption, and also DNA damages. As these compounds have great resistance to conventional treatment methods and biodegradation, alternative methods are sought for removing emerging pollutants from water.

2.2. Conventional methods of wastewater treatment

The conventional methods of wastewater treatment include physical, chemical and biological methods. The main aim of wastewater treatment is to remove organic compounds, solids, and nutrients from wastewater [10].

Biological treatment includes the application of living organisms for eliminating chemical contaminants. Generally, factors such as aeration, temperature, and pH should be controlled to maintain microbial activity. On the other hand, physical treatment contains separation or isolation of material from the mainstream. Methods like screening, skimming, and sedimentation are applied to eliminate pollutants [10]. Chemical methods in wastewater treatment involve chemical precipitation, dechlorination, chemical reduction, and oxidation and other chemical reactions [11].

A common scheme of the wastewater treatment process includes preliminary, primary, secondary, tertiary steps. Preliminary process designed to eliminate large, floating and suspended solids. The primary step removes inorganic and organic solids by flotation and sedimentation processes. Generally, almost 65% of the incoming grease and oil, 25-50% biochemical oxygen demand and 50-70% of the total suspended solids are eliminated during primary treatment. The secondary treatment step involves processes applied to eliminate suspended solids and residual organics after primary treatment. It contains biological wastewater treatment processes by using various types of microbes in a controlled condition [12].

Finally, tertiary wastewater treatment includes a series of supplementary steps after secondary treatment to reduce the concentration of metals, turbidity, nitrogen, and phosphorus by performing one of the following processes: reverse osmosis, coagulation, adsorption of

organics by activated carbon, filtration. This treatment is commonly implemented when effluent is reapplied for recreational purposes and irrigation [13].

Primary and secondary treatments are considered as essential steps in wastewater treatment. These steps help to remove the largest part of suspending solids and biochemical oxygen demand. However, these steps might be insufficient to offer reusable water for domestic and industrial recycling. Therefore, supplementary treatment steps included wastewater treatment plants to further eliminate organic substances, solids, toxic materials and nutrients [12].

2.3. Advanced Oxidation Processes

Advanced Oxidation Processes (AOPs) are water treatment technologies based on mineralizing and degrading recalcitrant organic pollutants from effluent using hydroxyl radicals [14]. Generation of free radicals play key roles, as the efficiency of advanced oxidation processes depends on them. Free radicals are molecules or atoms that can exist independently and have one or several unpaired electrons. They are peroxide ($O_2^{\cdot -2}$), superoxide radical ($O_2^{\cdot -}$), hydroxyl radical ($HO^{\cdot}$). Among all these radicals, the hydroxyl radicals play a key role in advanced oxidation processes [15]. When advanced oxidation processes are implemented for wastewater treatment, free radical species as oxidizing agents, destroy wastewater contaminants and transfer them to less or even non-toxic compounds [16]. Hydroxyl radicals ($OH^{\cdot}$) are considered as effective oxidizing agents in destructing organic substances. They are reactive electrophiles that react non-selectively and quickly with other organic substances. They possess an oxidation potential of 2.33V and oxidation reactions proceed with faster rates in comparison with conventional oxidants such as potassium permanganate and hydrogen peroxide [17]. The hydroxyl radical removes a hydrogen atom from organic substance (R-H) and generates an organic radical ($^{\cdot}R$). This radical undergoes a sequence of chemical reactions to produce various products and by-products. Organic pollutants theoretically should degrade to water and carbon dioxide by implementing advanced oxidation processes [10]. According to *Table 2.1,* the best results are achieved for the hydroxyl radical (•OH) and oxygen atomic.

$$^{\cdot}R - H + HO^{\bullet} \rightarrow H_2O + R^{\bullet} \qquad (2.1)$$

Table 2.1: The oxidation potential of oxidants [17]

Oxidizing agent	**Oxidation potential (V)**
chlorine	1.27
ozone	2.08
hydrogen peroxide	1.78
oxygen atomic	2.42
chlorine dioxide	1.27
hypochlorite	1.49
oxygen molecule	1.23
hydroxyl radical	2.80

It was noted that by implementing AOP technologies, the concentration of the pollutant reduces the amount that ranges from a few hundred ppm to less than 5ppb [18]. Advanced oxidation processes have been suggested as a promising technology to treat emerging pollutants, such as personal care products and pharmaceuticals [14].

2.4. Zeolites for treatment of emerging pollutants in water

Zeolites are made up of an aluminosilicate, microporous framework that has a negative electrical charge which is required to equalize the framework charge by providing the exact amount of cations. They present solid compounds that are used for a wide range of applications including managing the contamination of the environment. Zeolites become efficient ion exchange materials for water softening, purification of radioactive cations from liquid nuclear waste, and removal of transitional metal cations from wastewater by replacing zeolite cations with other cations introduced into the solution phase [19].

The first zeolites were established by Cronsted in 1756, but their properties remained unexplored until the 1920s. Additionally, because of the unsuitability of natural zeolites for commercial consumption, their development was delayed for some time. For this reason, researchers have begun to study the use of chemicals and minerals such as coal ash and others for the synthesis of synthetic zeolites. Natural zeolites are produced in the form of crystals on the surface of basalt rocks for several years or from glass or volcanic tuff that changes due to interaction with salt water. Synthetic zeolites are the product of the chemical process with a more uniform and pure composition of the pore size, the cages of framework and structure compared to the naturally obtained zeolite. The property of zeolites depends on the pressure,

temperature, amount of raw materials as Al_2O_3 and SiO_2, on aging period and activation process, pH, the concentration of the reagent solutions [20].

Zeolite structure contains three independent components: the aluminosilicate framework, water, and exchangeable cations. The chemical formula of zeolites is $M_{x/n}[Al_xSi_yO_{2(x+y)}]\cdot pH_2O$ where M is (Li, Na,K) and/or (Mg, Ca, Ba), n is cation charge; p/x=1-4, y/x=1-6. Tetrahedron is considered as main block of zeolite framework. The center is filled by an aluminuim and silicon atom and with four oxygen atoms at the vertices. Replacement of Si^{4+} by Al^{3+} forms the negative electrical charge on the lattice. The aluminosilicate framework is the most persistent component. The water molecules exist in voids of large cavities and bonded between exchangeable ions and framework ions through aqueous bridges. The main characteristic of zeolites is the capability of exchanging ions with external medium. Ion exchange process carries in an isomorphous fashion [21]. Currently, 235 different framework types of zeolite have been defined in synthetic and natural zeolites. Each of them named with a three-letter code by the International Zeolite Association. The frameworks of zeolites could be broken down into rings that have various sizes and serve as the pore opening windows of zeolites. Based on their biggest pore windows zeolites could be classified into the small pore (eight rings), medium pore (ten rings), large-pore (twelve rings) and extra-large pore zeolites (>twelve rings). Further species (e. g., water) in the zeolite pores could be eliminated, providing void space for guest species of the proper shape, size and polarity. It is known as the molecular-sieving effect of zeolites.

One of the most essential properties of zeolite is ion-exchange method. The exchange of ions proceeds by replacement of cation with another cation from the solution. Zeolite gives this property by substitution of silica ion (Si^{4+}) with aluminum (Al^{3+}) ion and forms a negative charge. This negative charge can be neutralized by various types of cations. Sodium (Na^+) ions are used as the neutralizing cation, this cation could be quickly replaced by other cations.

$$\boldsymbol{2NaZ + MgCl_2 = MgZ_2 + 2NaCl} \quad \text{Z – zeolite} \qquad (2.2)$$

The zeolites are applied as catalysts in industry. Approximately 99% of the world's petroleum that is obtained from crude oil depends on the zeolite application. Bronsted sites (active sites) form by the exchange of cations with ammonium hydroxide and are considered as the major reason zeolites applied as catalysts in industries. The hydroxyl groups produce inside the zeolite pore structure which possesses large electrostatic field attracting organic molecules. This causes bonds' rearrangement during chemical reactions.

Adsorption agent: Adsorption process occurs by cohering liquid molecules with a solid surface. The mixture of species can be separated by this process; also it depends on the

mixture affinity to the solid surface. The solid surface is referred to as adsorbent, adhering molecule is called as the adsorbate. The desorption process proceeds by removing the adhering molecule from the solid surface. It allows adsorbent to be reused.

Methods used in zeolite synthesis.

The production of crystalline state materials are categorized into two groups: reaction proceeds in liquid state and solid state. Reactions in the solid state are carried out above 300^0C to make easier the reactants' transportation to the sites. Reaction in the liquid phase occurs in the presence of a solvent. As in liquid phase transfer of molecules is easier than in solid phase, synthesis was carried out at lower temperature.

Hydrothermal method: This method is conducted in the presence of solvent (water), at the temperature range 90-180^0C. The synthesis is usually conducted inside a teflon-lined autoclave with pressure up to 15 bars. This method is considered as a much cheaper and easier method in comparison with others.

Solvothermal method: The synthesis includes using a solvent for zeolite production. Solvents such as pyridine, hydrocarbons, and alcohols are used. The type of solvents ranges from hydrophobic and nonpolar to polar and hydrophilic.

Ionothermal method: This method is carried out with ionic liquid and not molecular in nature. Ionic liquids are class of organic solvents with high polarity and a preorganized solvent structure. The examples of ionic liquids that are used for zeolite synthesis are 1-ethyl-3-methylimidazolium bromide (EMImBr), dialkylimidazolium bis(trifluoromethyl) sulfonyl]amides.

These solvents affect some properties such as low vapor pressure [22].

2.4.1. Applications of natural zeolites in wastewater treatment

Natural zeolites are abundant raw materials and exhibit ceramic properties even at elevated temperature phase transformations. They are crucial inorganic cation exchangers that present selectivity, high ion exchange capacity and compatibility with the environment. Aluminum (Al^{3+}) atoms are substituted over the silicon (Si^{4+}) in the zeolite framework by producing one negative charge on the framework. [23]. Zeolite supporting materials have been investigated as better candidates comparing with other supporting materials [24].

In general, zeolite is mostly used as a photocatalyst in conjunction with titanium dioxide (TiO_2), where it acts as a supporting material on which TiO_2 is doped. This is mainly because the catalyst enlarges the photocatalytic activity by high adsorption ability of zeolite. A review of research revealed that natural zeolites are successful supporters of TiO_2 for the

elimination of emerging pollutants. Nikazar et al. [25] prepared TiO_2 supported natural zeolite catalyst. In this investigation, the maximum photodegradation effect was observed by using 10 wt.% TiO_2, 90 wt.% clinoptilolite. Degradation of azo dye Acid red 114 was achieved 92.5% in 5 hours; however, the photodegradation conversion of Acid red 114 reduces with initial concentration increase. As the initial concentration of dye increases, the large amount of dye molecules adsorb light and the photons are not able to reach the photocatalyst surface.

Wardhani et al. [26] and Liu et al. [27] investigated the ability of regeneration and reuse of the TiO_2/zeolite particles. The compound with natural zeolite and TiO_2 was made by Liu et al. [27] to remove humic acid from aqueous solution. The adsorbent was regenerated by the photocatalytic oxidation process. The regeneration and reuse steps were performed 5 times. The research showed the high effectiveness of the adsorption process of humic acid by TiO_2/natural zeolite. Humic acid removal by zeolite achieved 80% within 5 min, whereas only 20% of humic acid was removed by bare zeolite alone. The low adsorption performance of bare zeolite is related to its highly negative structural charges at pH=7. Also, humic molecules become negatively charged at pH>3. This indicates that the electrostatic attraction of zeolite with humic acid is negligible. Similar results were obtained by Wardhani et al. [26]. TiO_2-natural zeolite was prepared by impregnation method. The degradation of methylene blue achieved 98.25% in 50 min by using UV irradiation. It should be noticed that the degradation efficiency reduces for about less than 10% after four cycles.

Zeolites doped with transition metal ions keep up an interest as promising catalysts for the degradation of emerging pollutants. They can be used as host materials which provide ordinary ligand promising catalyst system, with numerous types of coordination for cations. Also, they have a cage structure comprised of orthoaluminate (AlO_4^{5-}) and orthosilicate (SiO_4^{4-}) ion structural units. Their pores can serve for separately locating cations. Furthermore, the sintering or growth of nanoparticles can be limited by the restricted pores sizes of zeolites even at elevated temperature. Metal clusters and ions can be immobilized by thermal treatment and ion exchange process [24]. Abidin et al. [28] synthesized Ag particles impregnated on zeolite X by impregnation method. Impregnation of Ag particles to zeolite affected BET surface area to increase. The methyl orange degradation was achieved 100% in 8 minutes. Also, low silver weight was required.

The researchers have discovered that photocatalytic activity of TiO_2 can be enhanced by doping transition metals since noble metals act as photogenerated electron acceptors. The photogenerated electrons from TiO_2 surface rapidly transfer to the Pt particles, resulting in electron-hole effective separation and enhancement of photocatalytic activity under UV light

irradiation. Huang et al. [29] synthesized Pt modified TiO_2 loaded on natural zeolite by sol-gel technique and photoreduction method to examine photocatalytic degradation of methyl orange. It can be seen that doping Pt considerably increased photocatalytic degradation of TiO_2-natural zeolite catalyst from 73% to 87.8%. The effect of catalyst concentration on methyl orange decolorization was examined at a range from 0.5 g L^{-1} to 6 g L^{-1}. It was obtained that with the catalyst concentration increase at a range from 0.5 g L^{-1} to 3 g L^{-1} the decolorization rate of methyl orange solution rose considerably from 59.2% to 90.5% and after that it reduced with the increase of the catalyst concentration. Although at a higher level of catalyst concentration the reactive sites increases, the solution became opaque and cloudy, which decline the light penetration and cause to the reduction of the availability of active sites.

Also, doping several types of transition metals enhances considerably the light adsorption in the bandgap of TiO_2 [30]. Castañeda-Juárez et al. [31] prepared TiO_2 catalysts doped with Cu, Fe and Cu/Fe supported on clinoptilolite for treatment of diclofenac from aqueous solution. Transition metal doping presents intermediate bands in the bandgap of TiO_2 enhancing the catalyst performance. It was observed that Cu doping can effectively decrease the band gap of TiO_2 by the existence of p-orbitals and functions as active electron traps to decrease electron-hole recombination. Fe^{3+} doping occurs oxygen vacancies on the TiO_2 surface, which causes the formation of hydroxyl groups on the surface improving the degradation of the pollutant under UV light. At higher initial concentration of diclofenac large amount of diclofenac molecules are physisorbed on the catalyst surface, consequently fewer sites provide production of hydroxyl radicals. Thus, the efficiency of diclofenac degradation reduces.

The studies also focused on the effect of the transition metal sulfides loaded in the zeolite, as several transition metal sulfides show optical and electronic properties such as photoconductivity and semiconductivity. Nezamzadeh-ejhieh et al. [24] applied NiS – clinoptilolite catalyst for photocatalytic degradation of furfural. The study was focused on several transition metal sulfides and the choice was NiS, as it has a lower band gap than other semiconductors and also is cheaper than TiO_2. In this study, NiS formed inside the channels of the clinoptilolite by ion exchange and precipitation method. To define the role of NiS – clinoptilolite catalyst in the photodegradation process, bare clinoptilolite, NiS and NiS-clinoptilolite were tested by furfural solution. It can be concluded that NiS and bare zeolite particles solely did not show significant degradation of furfural. NiS particles tended to aggregate and resulted in a decline of active surface sites. In the case of NiS incorporated

zeolite, regarding the pore size of zeolite, there are small particles of NiS on the zeolite that increase available active sites of catalyst.

Some studies have investigated the application of ammonium quaternary materials as modifiers of zeolites. These materials can be used to modify natural zeolite due to their low cost and high availability. Mirzaei et al. [32] synthesized modified zeolite using the hexadecyltrimethylammonium chloride for Acid red 18 elimination from water. The main drawback of the study was the catalyst's low adsorption capacity. The same result was investigated by Taffarel et al. [33]. Researchers designed the modification of natural chilean zeolite with cetyltrimethylammonium bromide (CTAB) to explore its efficiency to remove the sodium dodecyl benzene sulfonate (SDBS) from the water. The research faces the same problems such as negligible removal of pollutants and recovery of catalysts for reusability.

From the *Table 2.2*, it can be seen that the selection of optimum catalyst concentration and optimal conditions for the chemical reaction process are crucial, as they affect catalyst activity.

Table 2.2: Natural zeolites for the removal of emerging pollutants

Catalyst type	Catalyst concentration (mg L^{-1})	Preparation method of catalyst	Pollutant (mg L^{-1})	Removal type	Removal (%) of emerging pollutant	References
Clinoptilolite (Iranian natural zeolite)+TiO_2	40	solid state dispersion	azo dye Acid Red 114 (50)	UV+catalyst UV+TiO_2 UV+clinoptilolite	92.9% for 5 hour 47.1% 8.3%	Nikazar et al. [25]
Natural zeolite/TiO_2	2000	impregnation	methylene blue (20)	photodegradation	98.25% after 50min	Wardhani et al. [26]
Natural zeolite/TiO_2	1000	sol gel	humic acid (10)	adsorption	80% in in 5 minutes	Liu et al. [27]
Pt modified TiO_2 loaded on natural zeolite	2000	sol-gel	methyl orange (20)	photodegradation	86.2% after 30 min	Huang et al. [29]
TiO_2 catalysts doped	10000	photo/electr	diclofenac	photodegradation		Castañeda-

with Cu, Fe, and Fe/Cu supported on clinoptilolite zeolite		ochemical–thermal method	(10)	Cu-TiO_2/zeolite Fe-TiO_2/zeolite Fe/Cu-TiO_2/zeolite	89.5% 82.2% 84.3%	juárez et al. [31]
NiS+clinoptilolite	330	ion exchange	furfural (28)	photodegradation	50% in 4hour 53% in 5 hour	Nezamzadeh-ejhieh et al. [24]
Clinoptilolite (surfactant modified zeolite with hexadecyltrimethylammonium chloride)	20000	-	Acid Red 18 (25) (50) (75)	adsorption	low adsorption capacity	Mirzaei et al. [32]
Cetyl trimethylammonium Bromide with modified chilean zeolite	2500	ion exchange	sodium dodecyl benzene sulfonate (30.7)	adsorption	negligible	Taffarel et et al. [33]

Also, Nezamzadeh-Ejhieh et al. [24], Wardhani et al. [26] and Huang et al. [29] used hydrogen peroxide (H_2O_2) as oxidant and showed that addition of an adequate amount of hydrogen peroxide is beneficial to the formation of hydroxyl radicals. Modification of catalysts that have reusability property is a crucial factor in the practical application of catalysts. Wardhani et al. [26] and Liu et al. [27] examined the reusability of TiO_2/zeolite 5 and 4 times respectively and found out that there are no significant decreases in the adsorption capacity. However, from *Table 2.2* it can be seen that the high amounts of catalysts were used.

2.4.2. Synthetic zeolites in wastewater treatment

Due to uniformity of particle sizes and purity synthetic zeolites are commercially applied more frequently than natural zeolites. The chemical reagents are considered the sources of synthesized zeolites. The essential priority of synthetic zeolites among natural zeolites is that they could be obtained with different pore sizes and chemical properties. Also, synthetic zeolites have high thermal stability. The traditional method of obtaining synthetic

zeolites includes mixing silica solution with aluminate solution by adding alkali hydroxides. The types of synthetic zeolites depend on the following factors: reaction mixture composition, nature of reactants, process temperature, reaction time, pH of the mixture. The reaction mixture composition contains inorganic cations, OH^-, silica to alumina ratio. Raising the Si/Al ratio influences the physical properties of the synthetic zeolites. OH^- alters the nucleation time by affecting the transfer of silicates from the solid phase to the solution. Inorganic cations balance the framework and influence the purity of crystals and product yield. The raw materials for synthetic zeolites could be organic and inorganic precursors. The organic precursors quickly combined the metals into the network whereas the inorganic precursors provided more hydroxylated surfaces. The temperature of the process is directly proportional to the crystallization rate of the material. The zeolite synthesis is conducted in an alkaline medium (pH>10). The crystallization parameter helps to minimize the other phases production and the needed time for obtaining a desirable crystalline phase [34].

Durgakumari et al. [35] synthesized TiO_2 supported HZSM-5. The catalyst was prepared by solid-state dispersion (SSD) method. TiO_2 supported HZSM-5 was obtained by the mixture of TiO_2 with HZSM-5 by using ethanol. The adsorption level of phenol was higher than the adsorption level of chlorophenol on using HZSM-5 catalyst lonely. Adsorption level of phenol under illumination was remained the same as in the dark, whereas adsorption of chlorophenol under illumination is considerably increased. The adsorption of both contaminants in the dark reduced by raising TiO_2 loading to HZSM-5. It is because the number of adsorption sites reduced by loading TiO_2 on HZSM-5. The adsorption levels of both contaminants under illumination were increased by loading TiO_2 on zeolite. The other method which applies 5A and 3X zeolite with nano – TiO_2 loaded under ultra violet light for the photocatalytic degradation of oxytetracycline (OTC) was explored by Zhao et al. [36]. The results illustrated that the adsorption ability of 13 X and 5A at neutral medium indicated 1497 and 654 mg/g respectively. The optimum for OTC removal from wastewater is considered 10 wt% TiO_2/13X and 15 wt% TiO_2/5A photocatalysts. Pan et al. [37] investigated the synthesis of TiO_2 doped low-silica X zeolite for the degradation of the pharmaceutical compound 17α-ethinylestradiol (EE2). EE2 removal efficiency using UV-TiO_2-LSX was higher (60%) compared with UV-TiO_2 and UV alone. Zhang et al. [38] investigated the synthesis of TiO_2/MoS_2 zeolite Y by ultrasonic-hydrothermal synthesis method. The photocatalytic activity of zeolite explored for removal of methyl orange from the aqueous solution under solar light irradiation and compared with Degussa P25. It was seen that the photocatalytic activity of the catalyst was enhanced by adding MoS_2 in comparison with TiO_2/zeolite.

FAU – type zeolites encapsulated with titania showed selective performance of photocatalytic degradation of charged pollutants in water. The selective degradation of charged substances was achieved as the result of the electrostatic repulsion of anionic substrates and the attraction of cationic substrates by the zeolites which charged negatively. The preparation of the hybrid zeolite – titania was occurred by the ion-exchange method. The cationic substrates illustrated higher degradation rates than anionic ones [39].

The modification of synthetic zeolites was also obtained by hexadecyltrimethyl ammonium bromide (CTAB) surfactant. Hashemi et al. [40] explored zeolite Y with CTAB and figured out that the most efficient catalyst was 50% of CTAB loading in zeolite Y. It can eliminate 89 % organic contaminants. The chemicals and minerals such as fly ash and coal ash are studied for synthetic zeolite synthesis. Gjyli et al. [41] synthesized zeolite through hydrothermal and fusion treatments from fly ash. The adsorption ability of synthetic zeolites was analyzed by the removal of phenol from aqueous solution. The conversion of phenol was achieved to 95%. Another method of converting coal fly ash (CFA) to Zeolite Y was demonstrated by Ren et al. [42]. Zeolite Y was synthesized by the alkali fusion hydrothermal method without any application of organic compounds. The catalytic activity was examined using acetone. The adsorption capacity of zeolite Y was achieved by 88.5% using after 6 cycles.

Table 2.3: Synthetic zeolies for the removal of emerging pollutants

Catalyst type	Catalyst concentration ($mg\ L^{-1}$)	Preparation method of catalyst	Pollutant (mg/l)	Removal type	Removal (%) of emerging pollutant	References
Zeolite HZSM-5/TiO_2	3000	solid state dispersion	phenol (0.235) chlorophenol (3.2)	UV+catalyst (phenol) UV+catalyst (chlorophenol)	88% 80 %	Durgakumari et al. [35]
5A and 3X zeolite with nano –TiO_2	200	solid state dispersion	oxytetracycline (50)	photodegradation 15%wt TiO_2/5A 10%wt $TiO_2$13X	90.11% 94.82%	Zhao et al. [36]
Zeolite X –TiO_2	-	Kuhl	*17α-ethinylestradiol*	photodegradation	60%	Pan et al. [37]

		method	(50)			
TiO_2/MoS_2 zeolite Y	125	ultrasonic-hydrothermal synthesis method	methyl orange (20)	photodegradation	96%	Zhang et al. [38]
FAU zeolite/titania	500	encapsulation	rhodamin (30)	photodegradation	40%	Zhang et al. [39]
Zeolite Y with CTAB	400	-	organic content	photodegradation	89%	Hashemi et al. [40]
Zeolite F type	200	pre fusion hydrothermal	phenol (30)	adsorption	95%	Gjyliet al. [41]
Zeolite Y	-	alkali fusion hydrothermal	acetone (80)	adsorption	88.5%	Ren et al. [42]

2.5. Fenton processes

This process is considered as the oldest method to eliminate toxic compounds in wastewater treatment. Formation of $OH^{\cdot}$ radicals by Fenton reagent take place by the addition of hydrogen peroxide to (H_2O_2) the soluble iron (II) salt.

$$Fe^{2+} + H_2O_2 = Fe^{3+} + OH^- + OH^{\cdot} \quad (2.3)$$

The process is determined as an attractive advanced oxidation process due to its reagents: hydrogen peroxide is environmentally friendly and iron is non-toxic and abundant element [43].

Ferrous ions and H_2O_2 are generally consistent in a strong acid environment. Redox reaction is conducted when H_2O_2 is added to the ferrous ions in a strong acid [44].

$$H_2O_2 + Fe^{2+} = Fe^{3+} + HO^- + HO^{\cdot} \quad (2.4)$$

$$HO^{\cdot} + RH = H_2O + R^{\cdot} \quad (2.5)$$

$$R^{\cdot} + Fe^{3+} = R^+ + Fe^{2+} \quad (2.6)$$

$$R^+ + H_2O = ROH + H^+ \quad (2.7)$$

Actually, the Fenton process has various crucial advantages for wastewater treatment:

i) Cheap chemicals and easy to manage

ii) Energy input is no needed

iii) Flexible process allows easier implementation in plants.

However, the following disadvantages of the process have been also shown:

i) High risks and cost as the result of hydrogen peroxide transportation and storage

ii) Requirement of large amounts of chemicals for wastewater acidification at pH 2-4 before treatment

iii) Aggregation of iron sludge

iv) The inability of whole mineralization because of the Fe (III) carboxylic acid complexes production, these complexes cannot be broken with $OH^{\cdot}$ [45].

The Fenton oxidation process performance depends on several factors, such as catalyst and hydrogen peroxide concentrations, pH, reduction from Fe^{3+} to Fe^{2+}, temperature. The reaction intermediates can reduce Fe^{3+} ion. On the other hand, there are some reaction intermediates that eliminate Fe^{3+} from the Fe^{2+}/Fe^{3+} cycle. The maximum catalytic activity of the Fenton oxidation process demonstrates at pH 2.8-3.0. At pH > 3 Fe^{3+} forms precipitation, $Fe(OH)_3$ and hydrogen peroxide destroys into H_2O and O_2. Also, Fe (II) complexes formation causes a reduction of Fe^{2+} concentration. Another important factor in the Fenton process is temperature. The kinetics of the process enhances by temperature increase, but it also triggers hydrogen peroxide decomposition into H_2O and O_2. The Fe^{2+} and hydrogen peroxide concentration can be fixed based on the initial pollutant concentration [46].

2.5.1. TiO_2 and Fe-doped TiO_2 photocatalysts

In the past 20 years, semiconductor materials such as ZnO and TiO_2 have been extensively studied. TiO_2 is commonly applied as a photocatalyst due to its stability, non-toxicity and low cost [47].

The photocatalysis mechanism could be explored as the interaction of semiconductor catalyst with light. At ambient temperature electrons of photocatalyst locates in the valence band. In the presence of light photons, electrons are excited from valence band to the conduction band and electron-hole pairs form [48].

Most of the emerging pollutants degrade by the heterogeneous photocatalysis process in the presence of a catalyst. The heterogeneous photocatalysis process is the process that depends on the hydroxyl radicals' formation and semiconductor used as a catalyst with UV light. TiO_2 is excited by the UV light wavelength of $\lambda \leq 400$ nm, electron-hole pairs are generated. By hole the hydroxyl radicals are formed that can eliminate pollutants in wastewater. Particularly, valence band holes (hv^+) and conduction band electrons (e^-_{cb}) are formed from UV illumination of TiO_2. The band electrons interact with molecular oxygen to produce anions of superoxide radical and band holes are interacted with water to form

hydroxyl radicals. The following equations show the mechanism of hydroxyl radical formation [49].

$$TiO_2 + h\nu \rightarrow e^-_{cb} + h^+_{vb} \quad (2.8)$$

$$e^-_{cb} + O_2 \rightarrow O_2^{\cdot-} \quad (2.9)$$

$$h^+_{vb} + H_2O \rightarrow OH^{\cdot} + H^+ \quad (2.10)$$

TiO_2/UV light is affected by several factors: catalyst weight, initial pollutant concentration, reactor's design, temperature, UV time, pH of solution and light intensity, in the existence of ionic species. The excess amount of catalyst may decrease the energy which is moved to the medium because of the catalyst particles' opacity. Reactor's design should provide uniform irradiation for catalyst surface. Temperature can affect the reaction rate and between 20 and 80°C, a negligible change of reaction rate has been reported. However, the temperature above 80°C a reduction of reaction rate has been noticed. pH of solution also affects the photocatalysis process. At lower pH, reaction rates raise for weakly acidic contaminants, however, at higher pH, reaction rates increase for contaminants that are hydrolyzed under alkaline conditions. The presence of ionic species affects the degradation process by adsorption of pollutants and UV light absorption [50].

Many studies are focused on enhancing the photocatalytic efficiency of TiO_2 in order to reduce the recombination rate between holes and electrons, improve interfacial charge transfer reactions. Therefore, TiO_2 is modified with metals, metal ion doping, nonmetal atoms [51]. Choi et al. [51] investigated 21 metal ion dopants to the TiO_2 and figured out that at 0.1-0.5% Fe^{3+} enhances photoreactivity for reduction and oxidation process and the removal of carbon tetrachloride was achieved 80%. Another investigation of synthesis 0.05% and 0.1% Fe-doped TiO_2 made by Vargas et al. [52], which used the sol-gel method at 200°C. The photocatalytic activity was tested for the degradation of phenol and dye Cbacron Yellow LS-R. The results show that synthesized catalysts have the same removal (83%) efficiencies as Degussa 25. Trovo et al. [53] studied caffeine degradation via the photo-Fenton process. The caffeine removal was reached 78%. Siciliano et al. [54] observed the degradation of caffeine with TiO_2 P25 and UV light for 120 minutes and figured out that total removal was reached within 15 minutes.

2.6. Removal of caffeine from aqueous solution

Caffeine has been applied in a large amount for different purposes and now has been found in the aquatic environment. In Brazil, the city of Campinas, tap water samples were

examined for 11 emerging pollutants. Among pollutants, caffeine was in third place with a concentration of 0.22 ± 0.06 μg L^{-1} [55]. In India, 15 pharmaceuticals, PPCPs were detected in the Ganges River. The concentrations of examined emerging pollutants in the river water ranged from 54.7 to 826 ng L^{-1}. Caffeine showed the highest concentration (743 ng L^{-1}) among them [56]. The study of the first national-scale assessment of emerging pollutants provides evaluation of microorganic substances in groundwater in Wales and England. Caffeine is categorized fourth (83.9%) by frequency of detection among 30 compounds [57].

Caffeine (1,3,7-trimethyl xanthine) is considered as a compound of the alkaloid group. It is extensively applied psychoactive drugs, which a constituent of food, beverages, medicines, and tobacco. This compound persists in the environment due to its high solubility in water and low octanol partition coefficient indicating the resistance to some treatment methods such as microbial degradation. *Table 2.4* illustrates the physical properties of caffeine [58].

Table 2.4: Physical properties of caffeine

Property	Value
Density	1.23 g/cm^3
Melting point	235 to 238^{0}C
Boiling point	178^{0}C
Solubility in water	2g/100 ml (at room temperature) 66g/100 ml (in boiling water)
Solubility in ethanol	1.5g/100ml
Octanol-water partition coefficient	K_{ow} = 0.01

The presence of emerging pollutants causes the degrading quality of coastal and inland waters. It also contributes to economic losses due to the close of commercial/ recreational areas [59]. For that purpose, the development of caffeine removal processes is needed. One of the methods which were applied by Gokulakrishnan et al. [60] for removal of caffeine was microbial method. Bacterial strains capable of degrading caffeine belonged to Pseudomonas and Serratia genus. Attempts were made for biological production of caffeine intermediates. However, this process proceeds relatively a long time. Caffeine removal was also conducted by using Mg-doped ZnO-Al_2O_3 heterostructure by Elhalil et al. [61]. The photocatalytic activity of the catalyst was assessed under ultra violet irradiation. The optimum dosages of catalyst and caffeine concentration were 20 mg L^{-1} and 0.3 g L^{-1} respectively. 1% Mg-ZnO-Al_2O_3 catalyst illustrated the highest photocatalytic efficiency (98.9%). However, efficiency was reduced by increasing Mg content. Zeolite supported catalysts were also

applied for the removal of caffeine. ZnO loaded zeolite catalyst was used for adsorption and adsorption/photocatalytic tests. In dark conditions, the removal of caffeine was 60% and in the presence of ultra violet light, it was achieved almost 95% [62].

2.7. The scope of the research

The purpose of the literature review was to review the wastewater treatment technologies, their advantages and drawbacks. It is clear from the research reviewed the lack of scientific knowledge for the treatment of emerging pollutants. The photocatalytic treatment of caffeine in aqueous solution has not been fully studied. The research was dedicated to obtaining catalytic and photocatalytic processes to treat wastewaters containing emerging pollutants. The preparation of Ag modified zeolites and Fe-doped TiO_2 materials were planned for the treatment of organic caffeine under UV light. 27 experiments were carried out to study the performance of the synthesized catalysts to remove caffeine from wastewater.

Chapter 3 – Materials and Methods

3.1. Materials

Natural Ukrainian zeolite (NZU) with a particle size range of 1-2.5 mm was purchased from "ZEOCEM" (Slovak Republik). Trisodium citrate dihydrate ($C_6H_5Na_3O_7*2H_2O$, 99% w/w), sodium chloride (NaCl, 99% w/w), silver nitrate ($AgNO_3$ 99% w/w) were supplied by Sigma-Aldrich and sodium borohydride ($NaBH_4$, 99.5% w/w) were purchased from Fisher Scientific. Ultrapure water was obtained from Milli-Q equipment. Caffeine as an emerging pollutant was obtained from Sigma-Aldrich with above 99% purity.

Based on the material certificate provided by the manufacturer chemical composition and porosimetry data of natural Ukrainian zeolite (NZU) – clinoptilolite were presented in *Table 3.1* and *3.2* below.

Table 3.1: Porosimetry data of natural Ukrainian zeolite

	Surface area	Pore volume	Average pore diameter
NZU	12.6 m^2/g	0.027 cm^3/g	5.8 nm

Table 3.2: Chemical composition of natural Ukrainian zeolite

Compound [%]	SiO_2	Al_2O_3	Fe_2O_3	TiO_2	CaO	MnO	Na_2O	FeO	SO_2
NZU	67.07	12.4	0.90	0.19	2.09	0.72	2.05	0.76	0.08

For synthesis of Fe-doped TiO_2 iron (III) chloride anhydrous ($FeCl_3$, 97% w/w) and ammonium iron (II) sulfate hexahydrate ($(NH_4)_2Fe(SO_4)_2$, 99% w/w) were purchased from Fisher Chemical. TiO_2 (99.5%) was obtained from Sigma-Aldrich.

For pH adjustment, two chemicals were used: hydroxide (NaOH, 97% w/w) and hydrochloric acid (HCl, 37% w/w). HCl and NaOH were supplied by Fisher Chemical. HPLC analyzer, acetonitrile (C_2H_3N, 99.8% w/w) solution and ultrapure water were used with a ratio of 40:60 w/w. Acetonitrile was purchased from Sigma Aldrich.

3.2. Preparation of caffeine solution

The stock solution of caffeine with a concentration of 300 ppm was prepared by dissolving in 1 L ultrapure water. 50 mL of this solution was used to prepare a desired concentration of 30 ppm of caffeine. HPLC analyzer showed 29±1 ppm of caffeine. The organic carbon of caffeine ($C_8H_{10}N_4O_2$, MW = 194.19 g mol^{-1}, carbon present = 49.48 % w/w) in the aqueous solution was 15.16 ± 0.62 mg L^{-1}, that is near the calculated theoretical value of 14.84 mg L^{-1}. The stock

solution was kept in the fridge at 5.6^0C.

3.3. Synthesis of catalysts

3.3.1. Synthesis of silver loaded zeolites

110 g Ukrainian natural zeolite was sieved using electro-mechanical shaker Test Sieve for obtaining particles with diameters ranging from 0.8-1.4 mm. The impregnation method was used for obtaining *Na_NZU* zeolite using 1 M NaCl solution. The modified zeolite was stirred with heating at 60°C in light and incubated for 3 days. The solution of zeolite was changed to a fresh NaCl solution for 3 days. The sample was washed with deionized water and then dried in a laboratory oven at 60℃ overnight. 10 g of the sample was kept in the desiccator. The ion exchange reaction was carried out by mixing 100 g of modified zeolite with 250 mL of 0.1 M $AgNO_3$, then this mixture was left in the dark at ambient temperature for 24 h. After 24 h the initial concentration of Ag^+ was measured and Ag^+- loaded zeolite was washed with deionized water 5 times until the solution became transparent. Then obtained mixture dried at 60℃ in an oven. 4 different samples were prepared from 100 g silver loaded zeolite. One fourth of silver loaded zeolite placed in foil-covered container and kept in a desiccator as *Ag^+_NZU*. The other 25 g filtered and dried in a laboratory oven for 2 h at *500°C* and labeled as *Ag_2O_NZU*. For obtaining *c_Ag^0_NZU* catalyst 25 g silver loaded zeolite was mixed with 0.5 M trisodiumcitrate dehydrate. All surface of zeolite was covered with 0.5 M trisodiumcitrate dehydrate and left for 1 hour in ice. After that, deionized water was used for washing the mixture until pH of the solution was reached 6.5 to 7.5. The mixture dried and filtered in an oven at 60℃ for 8 h. Then it was stored in the foil covered container and placed in a desiccator. The borohydride reduction method was applied for decreasing *Ag_2O* formation on the *Na_NZU* zeolite surface. The last 25 g of silver loaded zeolite was used for the preparation of *Ag^0_NZU* catalyst. At this point, 0.5 M sodium borohydride ($NaBH_4$) was added to silver loaded zeolite. The surface of zeolite was covered with sodium borohydride solution not less than 1 cm and kept 1 h in an ice. The solution was rinsed to eliminate unreacted salt until pH becomes neutral. The sample then dried for 8 h in an oven at 60℃ and stored in the foil - covered container for further use.

3.3.2. Synthesis of Fe - doped TiO_2 catalysts

Catalysts of TiO_2 doped with iron were synthesized with dopant concentrations of 0.5, 1, 2 and 4 wt.% using the wet impregnation method. 100 mL of ultrapure water was used for suspending 3 g of TiO_2 (P25). After that, the needed amount of $FeCl_2$ (precursor) was added. The mixture that obtained continuously stirred for 24 hours and washed with distilled water three

times to eliminate precursor and then the mixture was dried in an air oven at *80°C* for 12 h. The dried catalyst was ground in a mortar and calcinated in a muffle surface at 500°C for 6 h.

3.4. Experimental procedure

3.4.1. Adsorption/photocatalytic experiments

All experiments were conducted using a 500 mL caffeine solution. The initial concentration of caffeine was 30 mg L^{-1} for all experiments. The amount of silver loaded zeolite catalysts which were used for each experiment equal to 0.25 g. The solution and catalyst were put into the reactor and stirred with a magnetic stirrer for 2.5 h. Adsorption experiments were conducted in the dark condition, while photocatalytic experiments were carried out using an ultraviolet lamp with 254 nm. Each adsorption/photocatalytic experiment on the mineralization of caffeine lasted for 150 minutes. The samples were taken at 0, 15, 30, 60, 90, 120, 150-minute marks and sent to analysis.

Adsorption and photocatalytic experiments were conducted with caffeine initial concentration and Fe-doped TiO_2 catalyst with different concentrations amount equal to 30 mg L^{-1} and 0.25 g, respectively. The volume of treated caffeine solution was also 500 mL. The solution and catalyst were put into the reactor and stirred with magnetic stirrer for 2.5 h. The photocatalytic experiments were carried out using ultraviolet lamp with 365 nm. Each experiment lasted 150 minutes and samples were taken 0, 30, 60, 90, 120, 150 - minute marks.

3.4.2. Assessment of removal efficiency

The samples were taken by A Vitlab 1000 µL automated pipette. The treatment efficiency of catalysts was evaluated by using pH, Total Carbon (TC) and HPLC analysis. The TC analysis was performed using Multi N/C 3100 instrument by Analytik Jena AG (Germany). HPLC analysis was performed for the determination of caffeine concentration by HPLC Agilent 1290 Infinity II system instrument. For HPLC analyzer, the separation of catalyst from the solution was occurred by filtration using Agilent Captiva premium syringe filters with a pore size of 0.2 µm. For TC analysis, Agilent Captiva premium syringe filters were used for solution filtration. They contain 0.45 µm regenerated cellulose (RC) filter.

All pH measurements were conducted using a LE409 electrode by MettlerToledo. The initial and final pH of the solution was examined. *Table 3.3* illustrates the experimental conditions of the experiments.

Table 3.3: Experimental conditions

Parameters	Value
TC (mg L^{-1})	15.16
Caffeine concentration (mg L^{-1})	30
Silver loaded catalysts (g L^{-1})	0.5
UV lamp (W/ nm)	30 / 254
Total volume treated (ml)	500
Experiment duration (min)	150
Temperature	22-25
Flow rate (ml min^{-1})	400-500
Initial pH	6-7

Characterizations of catalysts were determined using X-ray diffraction (XRD, SmartLab automated multipurpose X-ray Diffractometer purchased from Rigaku), Transmission electron microscopy (TEM, Jeol JEM – 1400 Plus), Scanning Electron Microscopy (SEM, Auriga Cross Beam 540, Carl Zeiss) and X-ray fluorescence (XRF) spectroscopy (PANalytical Axios mAX). XRD helps to analyze the presence of a particular crystal lattice. Rigaku (SmartLab® X-ray) diffraction system was applied for obtaining XRD patterns. The system was implemented with Cu Kα radiation source (λ = 1.540056 Å) in the 2θ range from 10 to 90° with a scan rate of $0.02°\theta \cdot s^{-1}$. The elemental composition of zeolites was obtained by using XRF spectroscopy. For obtaining discs to XRF analysis each 0.9 g silver loaded zeolite samples were mixed with 3.06 g of Fluxona-FX-XOO-2-Lithium metaborate, 5.94 g of Fluxana-FX-X1OO-2-Lithium Tetraborate and 18 mg of FX-ADD. The mixture was heated at 1000 ° C for 20 minutes platinum crucible and cooled before the XRF analysis. For obtaining the image of the surface of the sample and two - dimensional projection of the sample SEM and TEM were used, respectively.

The removal efficiency was defined by *Equation 3.1*, where C_0 is the initial concentration and C_t is the concentration after *t* time:

$$\textbf{\textit{Removal efficiency}} = \left(1-\frac{C_t}{C_0}\right) * 100 \qquad (3.1)$$

3.4.3. HPLC Infinity II

The presence of caffeine in the solution was analyzed by HPLC analyzer 1290 Infinity II by Agilent Technologies. It is a separation technique that includes injecting a tiny volume of liquid into the column with particles diameter ranges of 3-5 micron. Due to the high pressure obtained from the pump, the sample components are going down to the column with a liquid. With the help of column packing components are divided from one another. The components are detected by detectors and their amounts are measured. The instrument is shown

in *Figure 3.1* and has 4 major parts.

Figure 3.1: HPLC equipment a) high speed pump b) multisampler c) multicolumn thermostat d) diode array detector

The first part of the equipment is a high speed pump. The pump pushes the liquid through the liquid chromatography with a definite flow rate at the range 1 to 2-mL min^{-1} range. The operating pressure of the pump can achieve between 6000-9000 psi [63]. The second part of the analyzer is multisampler. They can operate both microtiter plates and vials with efficiency maximum 1300 bar pressure. The module holds up 6144 samples. All sample movements are performed with Cartesian robot. It contains an X-Y-Z drive for optimizing positioning and catching for the sample trays. Before the analysis, the injection needle was washed with 40% (w/w) acetonitrile and 60% (w/w) ultra-pure water. The standard configuration of needle injection from the samples is arranged between 0.1 µL to 20 µL. The research was done by using 5 µL from each sample [64]. The next part of the equipment is a multicolumn thermostat (MCT G7116B). It contains 8 columns with 100 mm length. The temperature range of the multicolumn thermostat is between 4 to 110℃. Injected sample is being precooled or heated before goes to the column. The final part of the analyzer is diode array detectors. It can detect individual components of samples. As the optical system, UV-lamp is applied with the wavelength between 190-800 nm [65].

3.4.4. The Multi N/C 3100 equipment

The Multi N/C 3100 equipment purchased from Analytik Jena AG was used to analyze the amount of total inorganic carbon, nitrogen and total organic carbon in the samples.

Thermocatalytic high temperature oxidation process has occurred during the analysis. The process proceeds in the presence of a platinum catalyst. Each repetition appears by taking 250 µl. Firstly, the injection takes place by a syringe pump. After that, it goes to the quartz

combustion tube. This tube is filled with quartz wool, high-temperature mat, and a platinum catalyst. The temperature in the quartz combustion tubes goes up to 800℃. Oxygen is implemented as an oxidation agent. In the condensation coil transferred gas is cooled. By the separation process condensed water flows to the TIC condensation vessel. After that, the removal of corrosive gases is being proceeded and carbon dioxide gas is added to the Focus radiation Non-Dispersive Infrared detector. The total carbon concentration quantified by measuring the amount of produced carbon dioxide. TIC reactor is applied for detecting inorganic carbon concentration. The total nitrogen concentration is measured in ChD (electrochemical detector) and CLD (chemiluminescence detector) [66].

3.5. Reactor configuration

All experiments were carried out using photochemical reactors TOPT-II purchased from Toption Instrument CO., LTD illustrated in *Figure 3.2*. The reactors with 500 mL solution were operated in batch recycle mode. A magnetic stirrer was used to mix the solution.

Figure 3.2: Photochemical reactor TOPT-II

For photocatalytic experiments Long-Arc UV Lamps Source purchased from Toption Instrument CO., LTD were used. The following technical specifications are given in *Table 3.4.*

Table 3.4: The technical specifications of Long-Arc UV Lamps Source

Specifications	**Value**
Power	30W/500W
Simulative light source	UV-light
Unique features	Super stable kernel, operating interface is simple and easy
Wavelength	254 nm/365 nm
Application	Inside- illuminated photochemical reactor
Suitable capacity	500 ml
Power source	220 V

Chapter 4 - Results and Discussion

4.1. Characterization of catalysts

The morphology and structure of the catalysts were identified by XRD, XRF, SEM and TEM. All dimensions were recorded with Cu Kα radiation source (0.1549nm) in the 2θ between 10° to 90°. XRD spectra of Ag modified zeolites illustrate bands of diffraction peaks of silver at 32.2°, 26.6° and 38.2°. The characteristic peak at 32.2 is attributed to *AgO* and diffraction peak at 26.6° is illustrated Ag_2O. The peak at 38.2° in spectra of *Ag* modified natural zeolites is characterized *Ag* metal. This confirms the formation of *Ag* nanoparticles and the doping zeolites with silver.

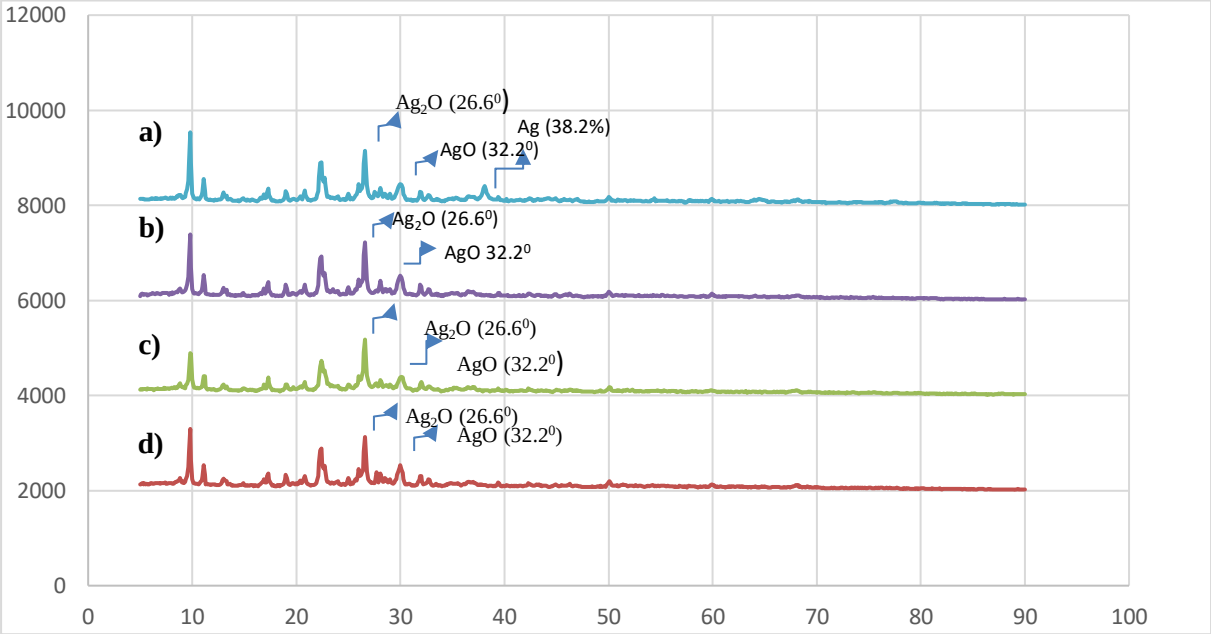

Figure 4.1: X ray diffraction patterns for Ag modified natural zeolites: a) Ag^0_NZU, b)c_Ag^+_NZU, c)Ag_2O_NZU, d)Ag^+_NZU

XRF analysis was applied to determine the chemical composition of zeolite samples. XRF analyses of silver modified zeolites were presented in *Appendix A*. Composition of *Ag* and Ag_2O presented in *Table 4.1* verified the success of loading zeolites with silver particles. The highest values were observed for the fourth sample *(Ag^0_NZU)*.

Table 4.1: XRF analysis results for Ag modified natural zeolites

Sample name	Ag (%)	Ag_2O (%)
Ag^+_NZU	2.17	2.34
Ag_2O_NZU	2.19	2.361
c_Ag^+_NZU	1.63	1.758
Ag^0_NZU	2.38	2.565

The chemical composition of Ag^0_NZU modified catalyst revealed that it was consisted of SiO_2 (77.098%), Al_2O_3 (10.994%), Na_2O (1.621%), MgO (0.210%) and SO_3 (0.055%), K_2O (2.318), CaO (0.754%), Ag_2O (2.565%), Fe_2O_3 (1.582%). The results confirmed the existence of silver as dopant in the sample and that silver was in its oxide form.

Table 4.2: The chemical composition of Ag^0_NZU

Compound	Concentration (%)
SiO_2	77.098
Al_2O_3	10.994
Na_2O	1.621
MgO	0.210
SO_3	0.055
K_2O	2.318
CaO	0.754
Ag_2O	2.565
Fe_2O_3	1.582

Elemental mappings (SEM/EDS) for all zeolite modified catalysts are showed in *Appendix B.* EDS provided information about the presented elements and their quantities. SEM images presented in *Appendix C*. SEM images of modified zeolites have porous structure and c_Ag^+ _NZU sample is more uniform than other modified zeolites. EDS mapping illustrates that the main structure of modified natural zeolite are oxygen, silicon and aluminum.

The TEM images of modified catalysts are shown in *Appendix D*. TEM images of modified catalysts showed that silver species are distributed as rounded in the surface of zeolites as dark spherical and rounded spots. Also, different size of silver species was being obtained. The first Ag^+_NZU sample has bigger species in size in comparison to other

samples, from the smallest 10.36 nm to the biggest 78.86 nm. The significant variance in size was not illustrated in other samples, usually from 8 to 30 nm. The formation of silver nanoparticles could be effected by several factors, such as temperature, concentration and nature of the reduction agent, pH. These factors have significant effect on the metallic phase nucleation and the reduction rate by affecting the distribution and size of the particles [67].

4.2. Direct photolysis using UV light

Initially, the direct effect of UV light on the caffeine solution treatment was explored. The initial concentration of total carbon was approximately 15-17 mg L^{-1}. The obtained results are illustrated in *Figure 4.2*. The treatment was carried out for 150 minutes and the obtained results indicated 4% conversion for TC removal. The obtained results of these experiments demonstrated that caffeine compound have high resistance to UV-light.

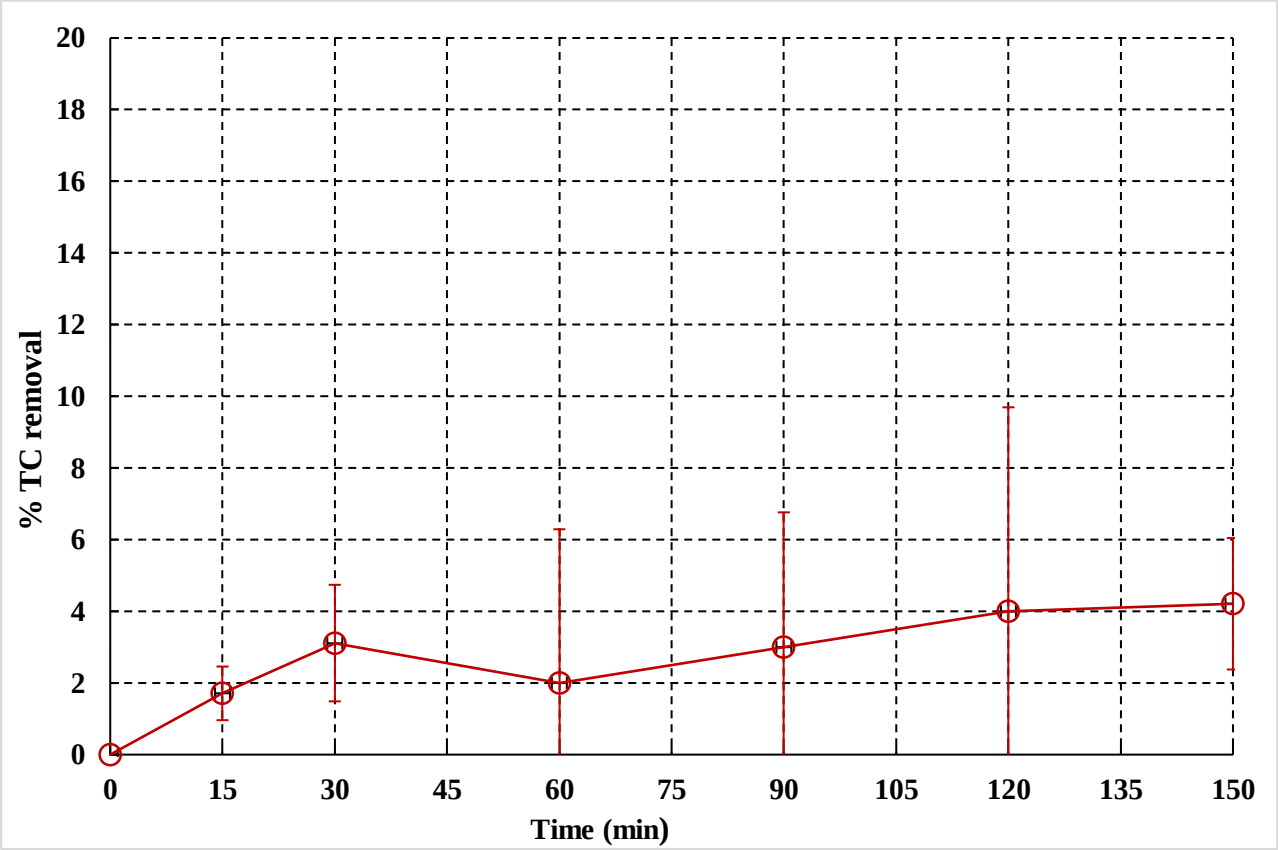

Figure 4.2: Direct photolysis efficiency on the treatment of caffeine TC removal (%)

The same result was obtained in other studies. Sacco et al. [62] showed that total carbon removal was 8 % after 240 min by the photolysis test. Therefore, it is important to design the process for the removal of total carbon from the caffeine solution. The novel adsorbents for caffeine removal should be designed to decrease their concentrations in water. The application of zeolites has taken a big attention due to their chemical and structural

properties. From the *Figure 4.3* it can be seen that the effect of direct photolysis on the caffeine degradation was not observed. The photolysis of caffeine under UV light 254 nm was reached approximately 7%.

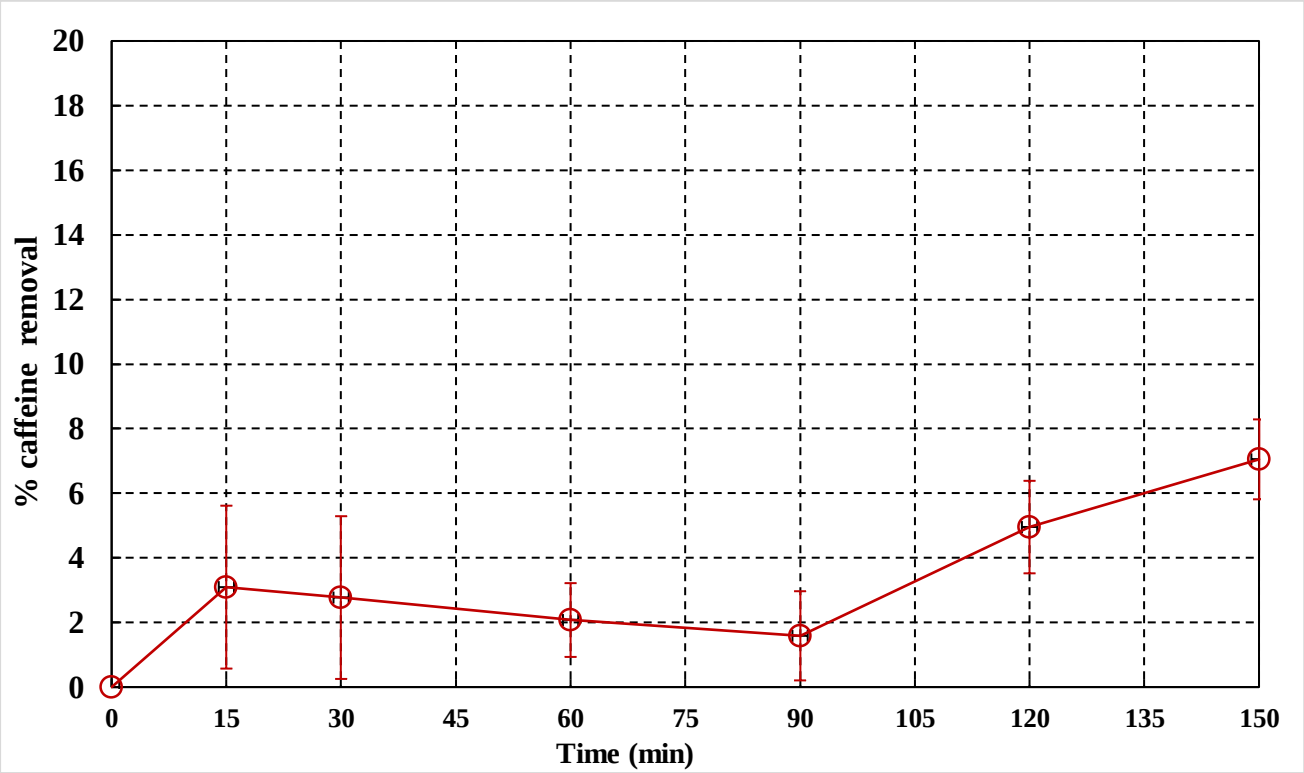

Figure 4.3: Direct photolysis efficiency on the treatment of caffeine. Caffeine removal (%)

Based on the literature, Tanji et al. [68] also found that the photolysis of the caffeine under UV light 272 nm was very low less than 2% after 2 h. Furthermore, Elhalil et al. [61] by using a UV mercury lamp (400 W) observed that the photolysis of caffeine was negligible. To conclude, caffeine cannot be significantly degraded by UV-vis irradiation and the treatment of waters contaminated with this substance needed a photocatalytic approach.

The overall reaction of photocatalytic degradation of caffeine can be given by *Equation 4.1*.

$$2C_8H_{10}N_4O_2 + 19O_2 = 16CO_2 + 10H_2O + 4N_2 \quad (4.1)$$

4.3. Adsorption experiments with silver modified zeolites

Caffeine can be derived into different compounds such as xanthine, 1-methylxanthine, 3-methylxanthine, 7-methylxanthine and others [69]. Therefore, these intermediates could be mistakenly taken with adsorption results done by zeolites. Also, they can decrease the concentration of caffeine in solution samples [70].

The findings performed by modified zeolites in dark conditions shown in *Figure 4.4.* In the beginning stage of adsorption, when the surface of modified zeolites are clear from the

caffeine molecules, the kinetics of adsorption is generally defined by the caffeine diffusion from the solution of bulk to the surface of modified zeolites. In the last stage of adsorption, the considerable number of caffeine molecules is adsorbed on the surface of modified zeolites and in this case the kinetics of adsorption lows down [71].

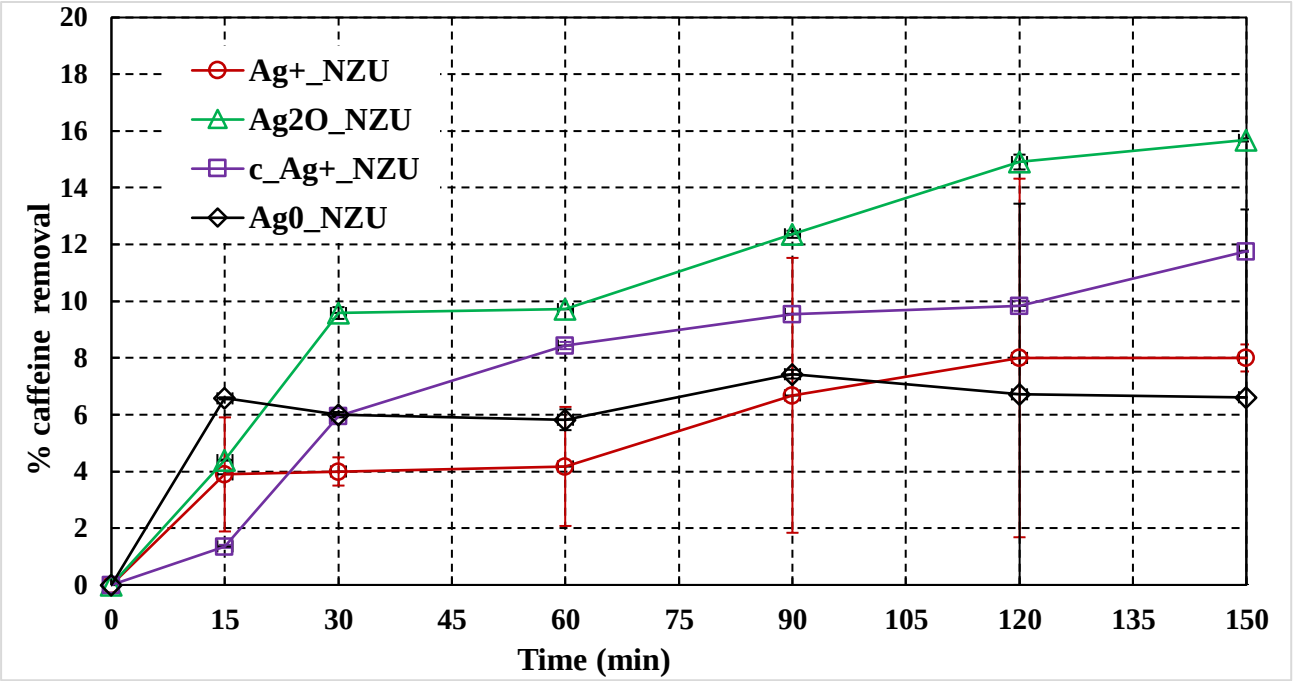

Figure 4.4: Adsorption process using modified zeolites

The obtained figure shows that in the presence of catalysts caffeine decreasing rate was moderately enhanced in comparison with UV radiation. The maximum caffeine removal (15.69%) was obtained by *Ag_2O_NZU* that possess 2.361% *Ag_2O* and 2.19% *Ag (Table 4.1)*. Other catalysts show caffeine removal in the range of 5 % to 10%. Korobeinyk et al. [72] also showed that I^- adsorption extraction rate raised by increasing silver content in modified zeolites and *Ag_2O_NZU* catalyst had the highest I^- removal.

Figure 4.5 provides results of total carbon (TC) removal using catalysts. It can be observed that TC removal of caffeine has fluctuating trends for each catalyst. The figure also illustrates that *Ag_2O_NZU* catalyst has the highest total carbon removal (10%) in comparison with other catalysts. TC removal by *Ag^+_NZU* was obtained 7%. The lowest TC removal showed silver modified catalysts *c_Ag^+_NZU* (3.46%) and Ag^0_NZU (3.625%) catalysts.

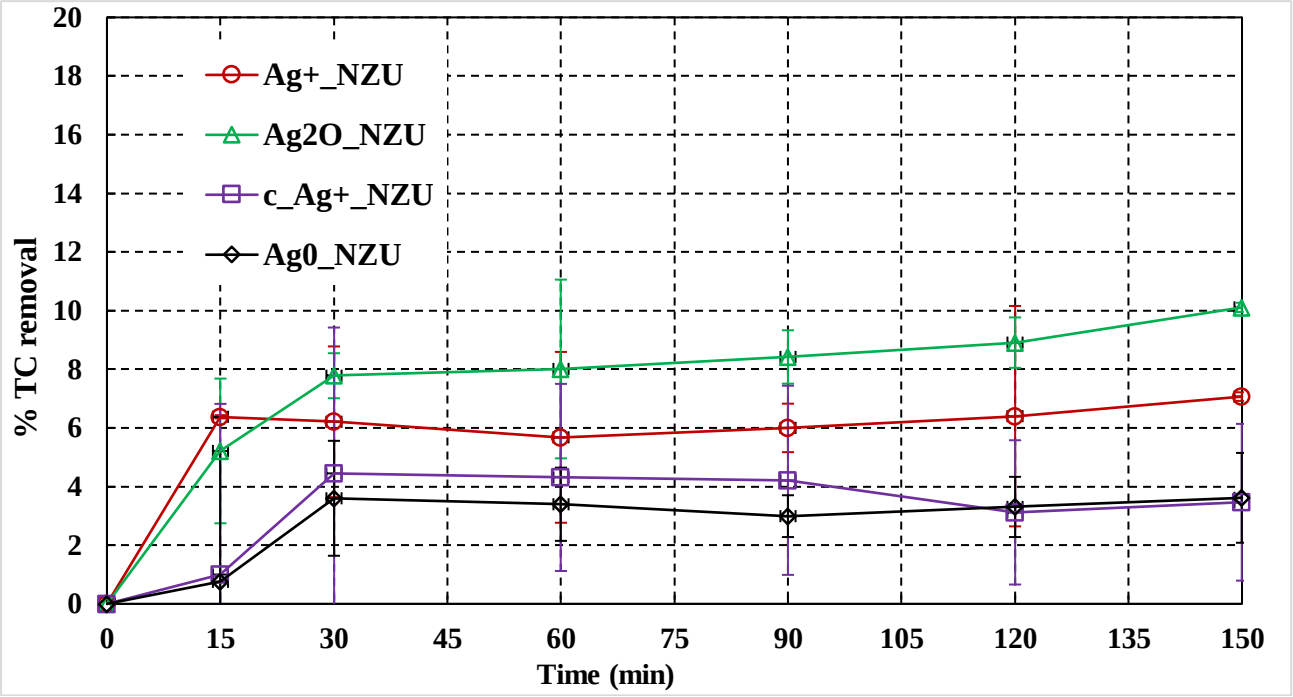

Figure 4.5: TC removal using catalysts

4.4. Photocatalytic treatment of using UV and silver modified zeolites

In Ag doped photocatalyst Ag-X, the Ag receives the photo-generated electrons as shown in *Equation 4.2* and reacts as electron-hole traps (*Equation 4.3-4.4*) that hinders the recombination observed in *Equation 4.5*. This occurs from the effective electron-hole pairs separation, the formation of $OH^{\bullet}$. The process represents in *Equation 4.6-4.7*. From the literature reviewed it is clear that the dopant effect does not enhance proportionally with doping percentage because above optimum amount dopant has structural instability of the host catalyst and crystal lattice [73].

$$Ag^{n+} + e^{-}_{cb}\,(X) \rightarrow Ag^{(n-1)+} \quad \text{(Reduction) (Electron trap)} \qquad (4.2)$$

$$Ag^{(n-1)} + X^{m+} \rightarrow Ag^{(n)+} + X^{(m-1)+} \qquad (4.3)$$

$$Ag^{n+} + h^{+}_{vb}\,(X) \rightarrow Ag^{(n+1+)} \quad \text{(Oxidation) (Hole trap)} \qquad (4.4)$$

$$e^{-}_{cb}\,(X) + h^{+}_{vb}\,(X) \rightarrow X \quad \text{(Recombination)} \qquad (4.5)$$

$$Ag^{(n-1)} + X^{m+} \rightarrow Ag^{(n)+} + X^{(m-1)+} \qquad (4.6)$$

$$Ag^{(n+1)} + OH^{-} \rightarrow Ag^{(n)} + {}^{\cdot}OH^{\bullet} \qquad (4.7)$$

Secondly, the degradation of caffeine under UV light and modified zeolites was studied. *Figure 4.6* illustrates that the photocatalytic process has no substantial effect on the caffeine removal, however from it can be seen that Ag^{0}*_NZU* and *c_*Ag^{+}*_NZU* have better performances among other modified catalysts.

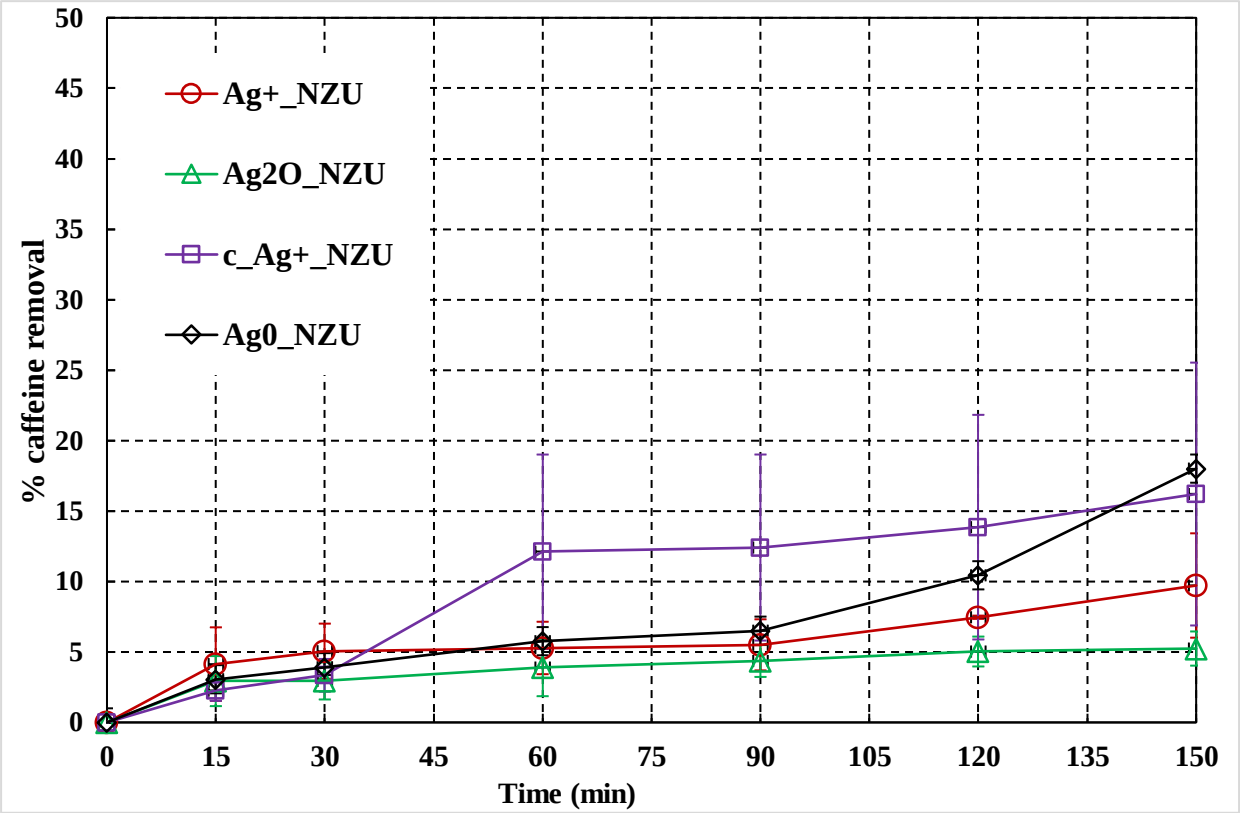

Figure 4.6: Caffeine removal using UV and Ag modified zeolites

It can be observed that *Ag^0_NZU* catalyst has the highest performance approximately 18%. The result shows that caffeine removal was increased in the presence of UV irradiation by using *Ag^0_NZU* catalyst. The catalyst has the highest silver content 2.38% *Ag* and 2.565% *Ag_2O* (*Table 4.1*). Furthermore, Vaiano et al. [74] noted that the photocatalytic activity of *Ag* modified catalyst was increased by increasing the metal content on the catalyst surface. This performance could be explained that noble metal nanoparticles perform like sinks for the photogenerated electrons, which result in slowing down of electron-hole recombination. This results in the enhancement of photoactivity improvement. Therefore, the covering of catalyst surface with noble metal particles can enhance photogenerated carrier's separation efficiency and increase catalyst photocatalytic activity.

From *Figure 4.7* it can be observed that TC value decreased with time. The TC removal increased in Ag modified zeolites such as *Ag^+_NZU* , *c_Ag^+_NZU* and *Ag^0_NZU* catalysts. TC removal of caffeine using *Ag^0_NZU* with UV light showed better performance (14.25%) in comparison with using *Ag^0_NZU* (3.625%) without UV light. *Ag^+_NZU* catalyst and *c_Ag^+_NZU* catalyst showed the same TC removal (approximately 10%). From *Figure 4.6* and *Figure 4.7* it can be observed that the highest photocatalytic degradation was observed by *Ag^0_NZU* catalyst.

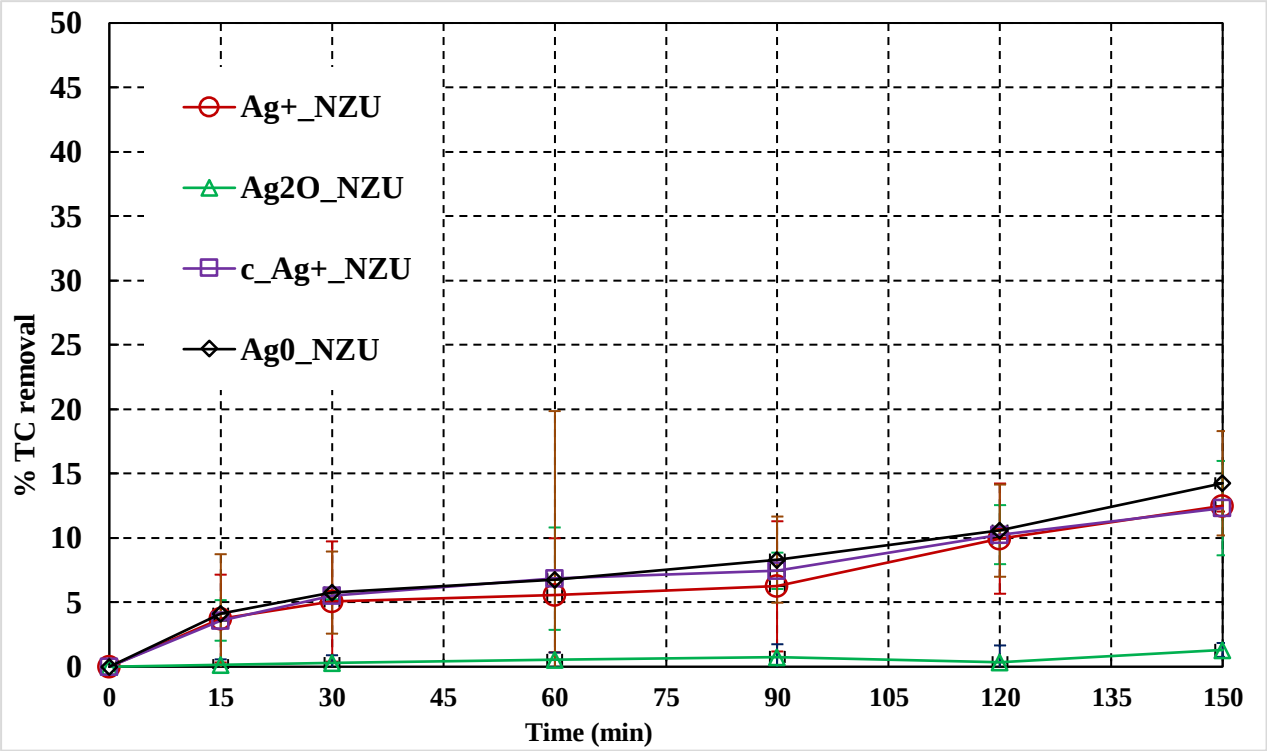

Figure 4.7: TC removal of caffeine using UV and Ag modified zeolites

As it was mentioned the photodegradation of caffeine is not completely studied. Various studies have been done to study caffeine photodegradation and studying derived compounds: 1,3-dimethylxanthine, 1,7-dimethylxanthine, 3,7-dimethylxanthine, 1-methylxanthine, 3-methylxanthine, 7-methylxanthine, xanthine [69]. The results obtained during the research did not meet expectations based on the previous studies. However, it is important to underline that zeolite which was used in the research natural zeolites that are not commonly used. The initial and final pH value of the solution for each experiment was measured. The difference in pH value between the initial and final solution was negligible. For the adsorption process, the average pH value was 8.61. The value was decreased from an average value of 8.61 to 8.04.

4.5. Photocatalytic treatment of caffeine with TiO_2

TiO_2 catalyst (P-25) was used as a main catalyst for evaluating the performance of Fe-TiO_2 catalyst with different concentrations of dopants. Three experiments with TiO_2 under ultraviolet light 365 nm were conducted. Ultraviolet light was absorbed by titanium dioxide semiconductor and forms hydroxyl radicals. The following chemical reactions show the generation of hydroxyl radicals [75]:

$$TiO_2 + h\nu \rightarrow e_{cb}^- + h\nu_{vb}^+ \quad (4.8)$$

$$ecb^- + O_2 \rightarrow O_2^{-\cdot} \quad (4.9)$$

$$hvb^{+} + H_2O \rightarrow OH^{\cdot} + H^{+} \qquad (4.10)$$

The analysis performed on total carbon concentration showed that TiO_2 catalyst with UV light 365 nm showed higher TC removal (26.72%) than UV light 365 nm without catalyst (4.21%). *Figure 4.8* illustrates the TC removal of caffeine using TiO_2/UV light.

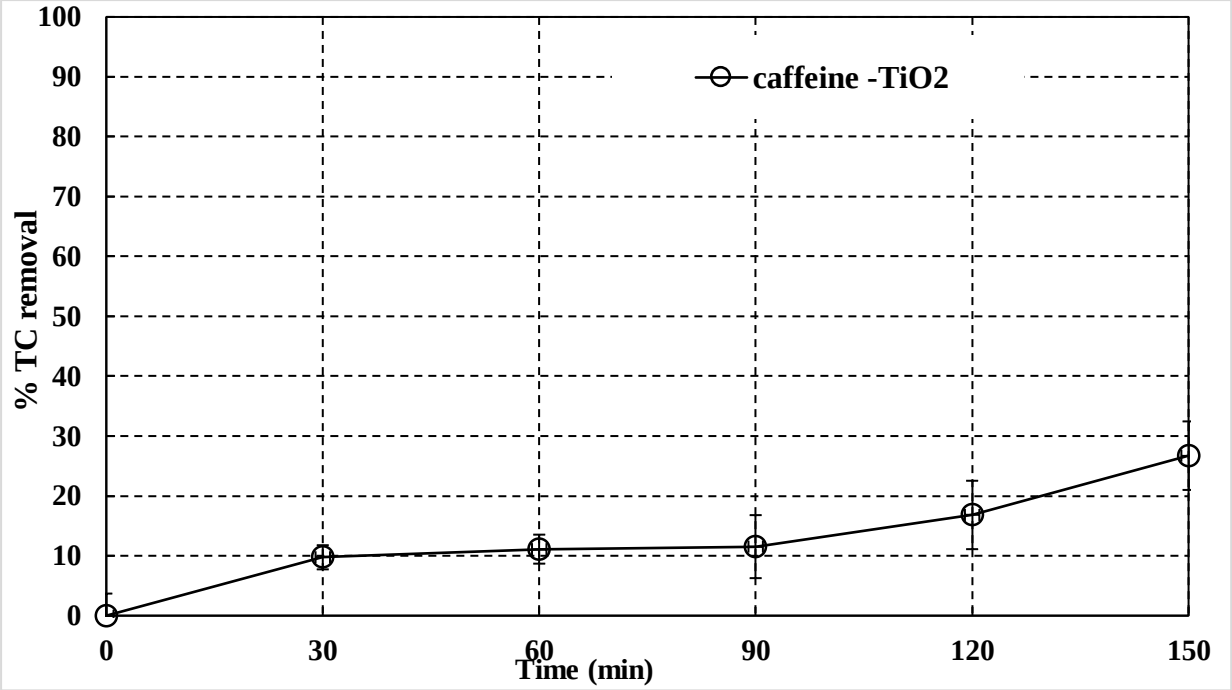

Figure 4.8: Total Carbon (TC) removal of caffeine using TiO_2/UV

For photocatalytic treatment of caffeine solution TiO_2 (P25) was used. TiO_2 photocatalytic activity depends on surface area, band gap, crystal composition (rutile and anatase phase), particle-sized distribution and surface hydroxyl density [76]. TC removal increased slowly; however, the caffeine removal was achieved 100% after 150 minutes. *Figure 4.9* shows caffeine removal using TiO_2 under ultraviolet light 365 nm.

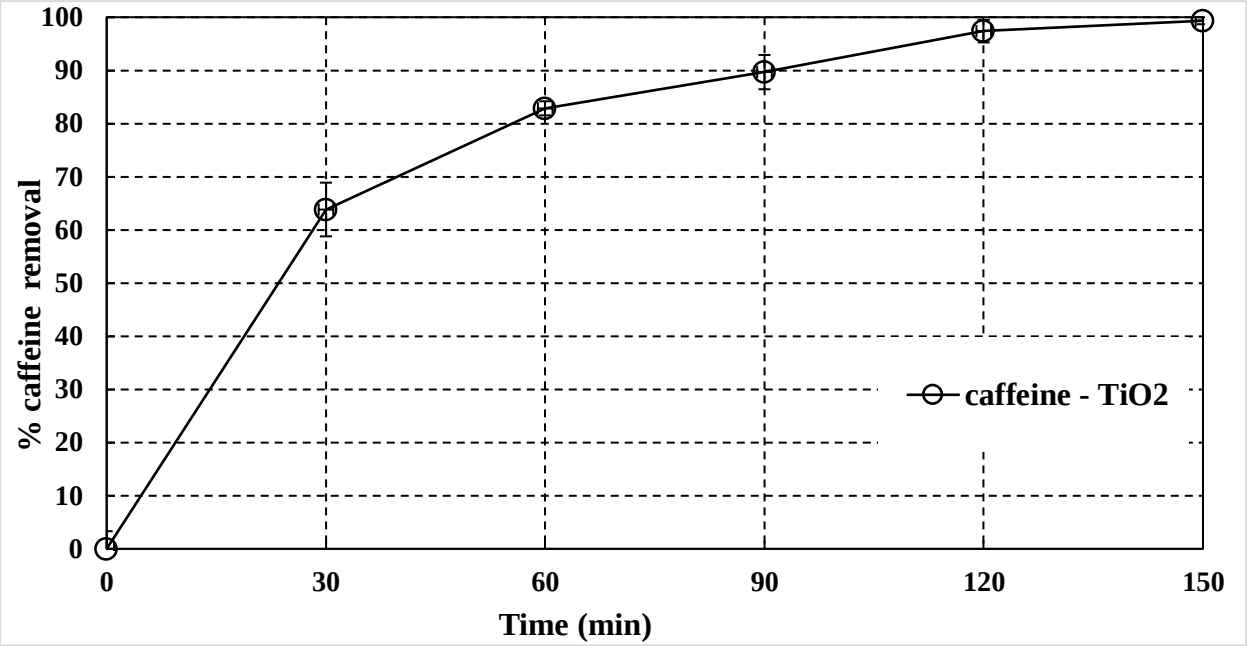

Figure 4.9: Caffeine removal using TiO_2/UV

Bouanimba et al. [77] studied TiO_2 (Degussa P25) in crystalline form (rutile) and obtained the decrease of caffeine concentration just to 10%. The authors noted that this is because of its crystalline form. TiO_2 (Aeroxide P25) that was used in this research is the combination of anatase/rutile phase and is considered as efficient photocatalytic material.

4.6. Photocatalytic treatment of caffeine using Fe-doped TiO_2

Iron particles as dopants have favorably effect to TiO_2 photocatalytic activity, this is due to the function of iron particles which acts as h^+/e^- traps. Thus, particles impede the recombination rate and enhance the photocatalytic activity. TiO_2 is excited by UV light and electron-hole pairs are generated *(Equation 4.11)*. Particularly, valence band holes (hv^+) and conduction band electrons (e^-_{cb}) are formed from UV illumination of TiO_2. Band electrons interact with Fe^{3+} and generate Fe^{2+} ions *(Equation 4.12)*. Fe^{4+} and Fe^{2+} are relatively unstable as compared to Fe^{3+}. Therefore, it is tendency for the transfer of the trapped charge carriers from Fe^{4+} and Fe^{2+} to the adsorbed O_2 and OH^-, respectively to form Fe^{3+} *(Equation 4.13-4.16)*. These produced active species ($OH^{\cdot}$ and $O_2^{-\cdot}$) will initiate the following photocatalytic reactions [78].

$$TiO_2 + hv \longrightarrow hv^+_{vb} + e^-_{cb} \quad (4.11)$$

$$Fe^{3+} + e^-_{cb} \longrightarrow Fe^{2+} \quad (4.12)$$

$$Fe^{2+} + O_{2(ads)} \longrightarrow Fe^{3+} + O_2^{-\cdot} \quad (4.13)$$

$$Fe^{2+} + Ti^{4+} \longrightarrow Fe^{3+} + Ti^{3+} \quad (4.14)$$

$$Fe^{3+} + hv^{+}_{vb} \longrightarrow Fe^{4+} \quad (4.15)$$

$$Fe^{4+} + OH^{-} \longrightarrow Fe^{3+} + HO^{\cdot} \quad (4.16)$$

Photocatalytic degradation of caffeine by Fe-doped TiO_2 was assessed by TC (*Figure 4.10*) and HPLC (*Figure 4.11*) analysis.

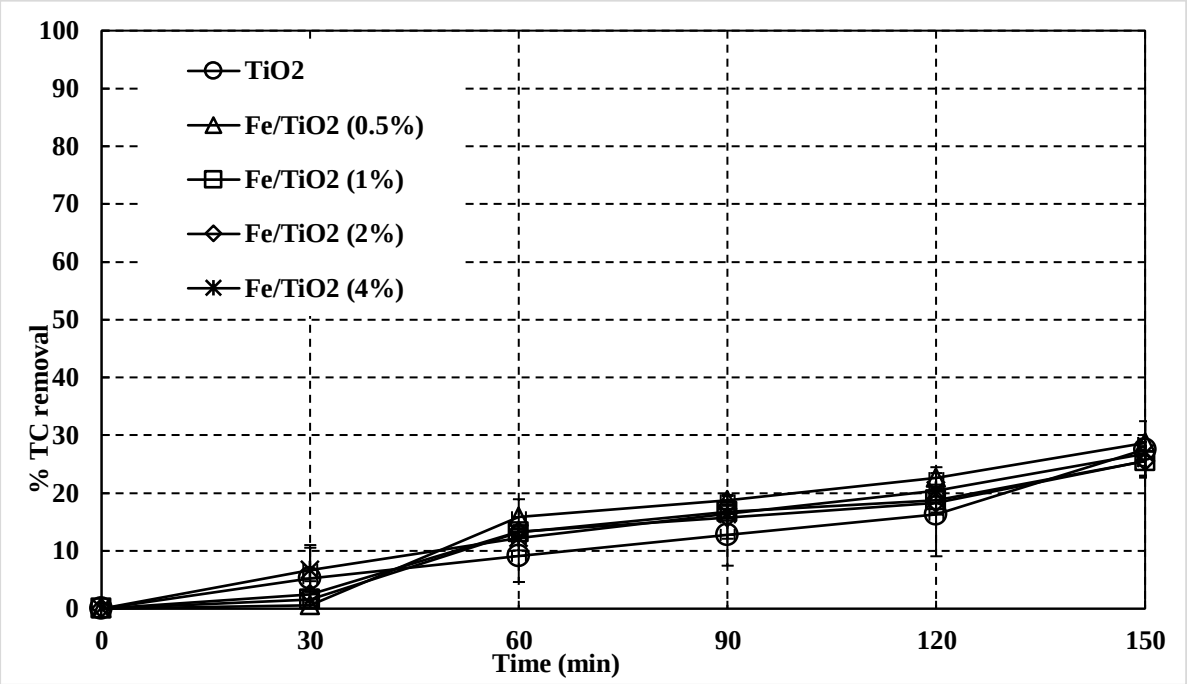

Figure 4.10: TC removal of caffeine by UV/TiO_2 and UV/Fe/TiO_2

It can be seen that TC removal value increased with time. After 150 minutes TC removal was achieved 27.55% by UV/TiO_2 process. The TC removal results using UV/TiO_2 was similar to using UV/Fe-doped TiO_2 catalysts. Vargas et al. [79] also showed that Fe-doped TiO_2 catalysts had similar TC removal efficiencies to the commercial photocatalyst Degussa P-25 TiO_2 for Yellow Cibacron LS-R. The authors reported that Yellow Cibacron LS-R has less photodegradation due to its molecular structure complexity and higher molecular weight. However, Zhu et al. [80] reported that under UV radiation 0.40% Fe-doped TiO_2 is more photoactive than TiO_2 (Degussa 25).

The mineralization of caffeine was effectively occurred by using all catalysts.

Figure 4.11 illustrates the caffeine removal using UV/TiO_2 and UV/Fe- doped TiO_2.

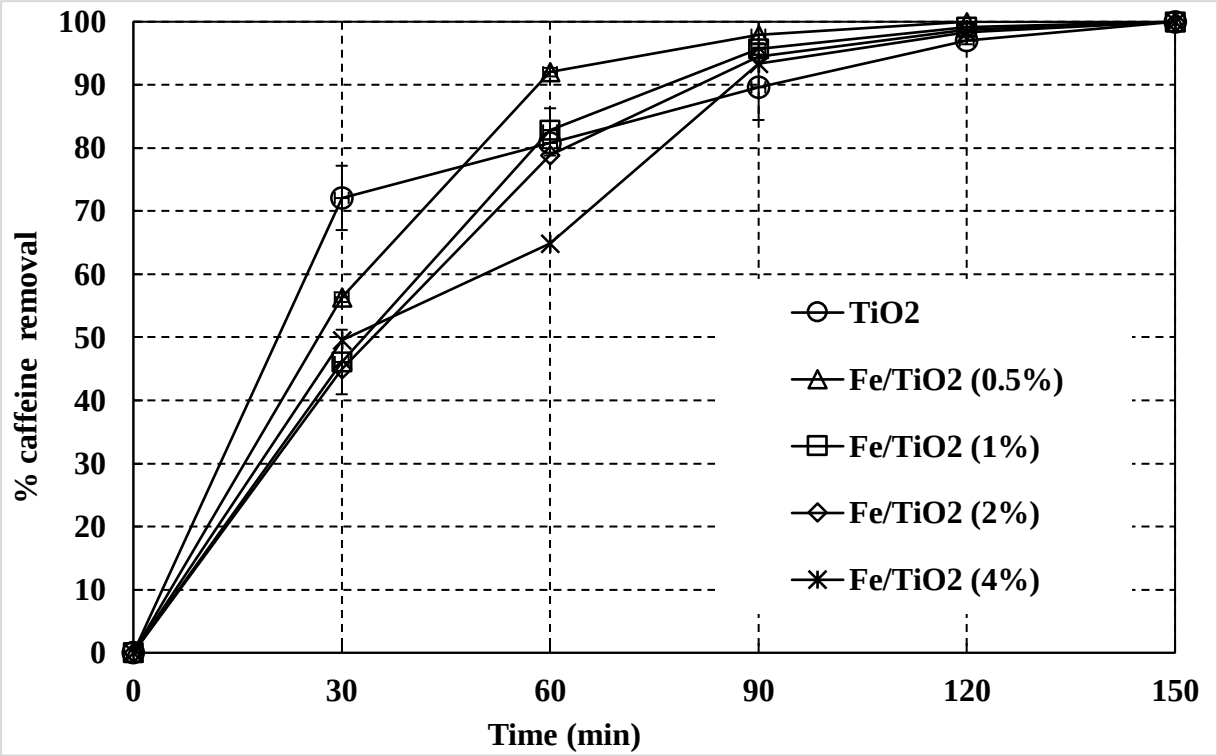

Figure 4.11: caffeine removal by UV/TiO2 and UV/Fe-TiO2

All catalysts were achieved 100 % caffeine removal. It can be observed from HPLC analysis that caffeine removal is higher than TC removal which was obtained from TC analysis. This can be explained due to the formation of reaction intermediates and not direct carbon dioxide formation. Therefore, even if caffeine is no longer in the solution, its intermediates present in the solution and cause the low degree of TC removal. A low degree of TC removal can be also explained by the occupation of active sites by organics [81].

The initial pH for caffeine solution varied from 7.10 to 7.69 for all experiments and the change in pH throughout the experiment was also measured and shown in *Figure 4.12*. The initial pH was around 7.10-7.69 and it decreased to about 6.5 at the end of the experiments. The rate of caffeine decomposition increases with decreasing pH value.

Andreozzi et al. [82] reported that the pH of the solution affects photocatalytic degradation. For weakly acidic pollutants at lower pH and contaminants that hydrolyze in alkaline solution, the photocatalytic degradation can be increased. The pH of caffeine solution was decreased by the time and achieves 6.5.

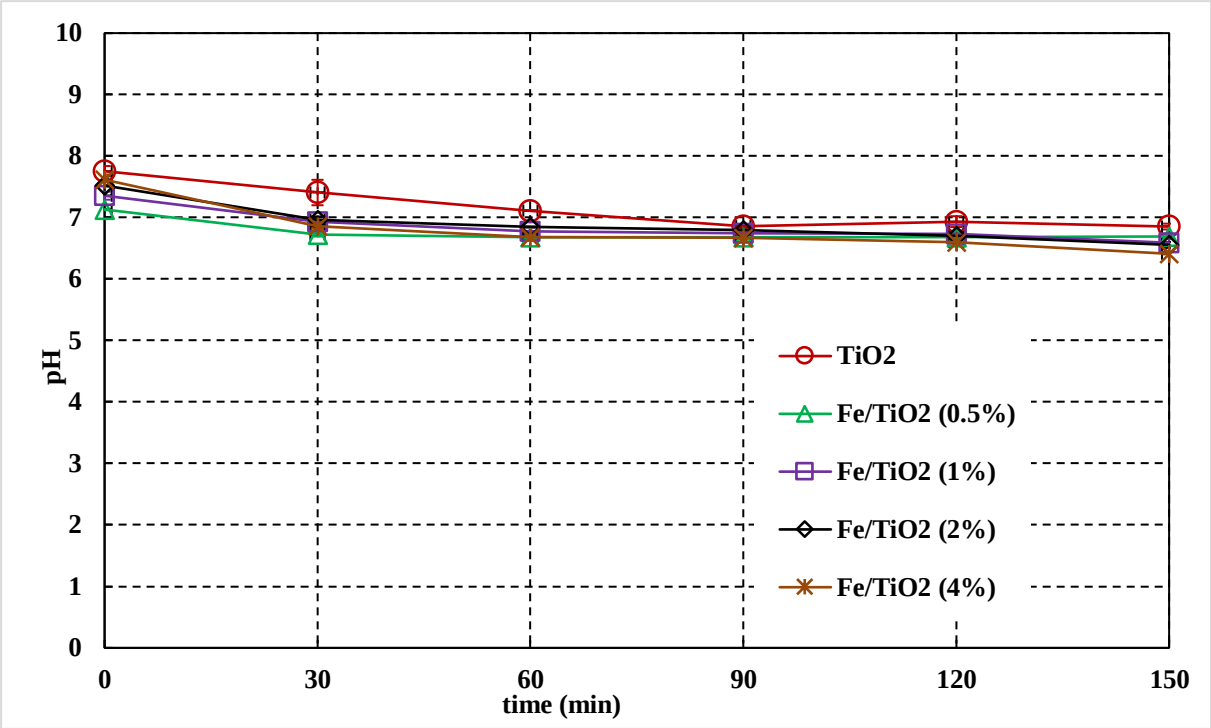

Figure 4.12: pH values throughout UV/TiO₂ and UV/Fe-TiO₂ processes

4.7. Energy consumption of experiments using UV/TiO₂ and UV/ Fe-doped TiO₂

The kinetics of caffeine degradation was investigated by testing a pseudo-first-order and pseudo-second-order kinetic models. The following equations were applied

$$\frac{ln\, C_t}{C_0} = -k_1 t \qquad (4.18)$$

$$\frac{1}{C_t} - \frac{1}{C_0} = -k_2 t \qquad (4.19)$$

Where k_1 *and* k_2 are reaction rate coefficients. The pseudo first order and pseudo second order kinetic models were shown in Figure 4.14 and 4.15, respectively.

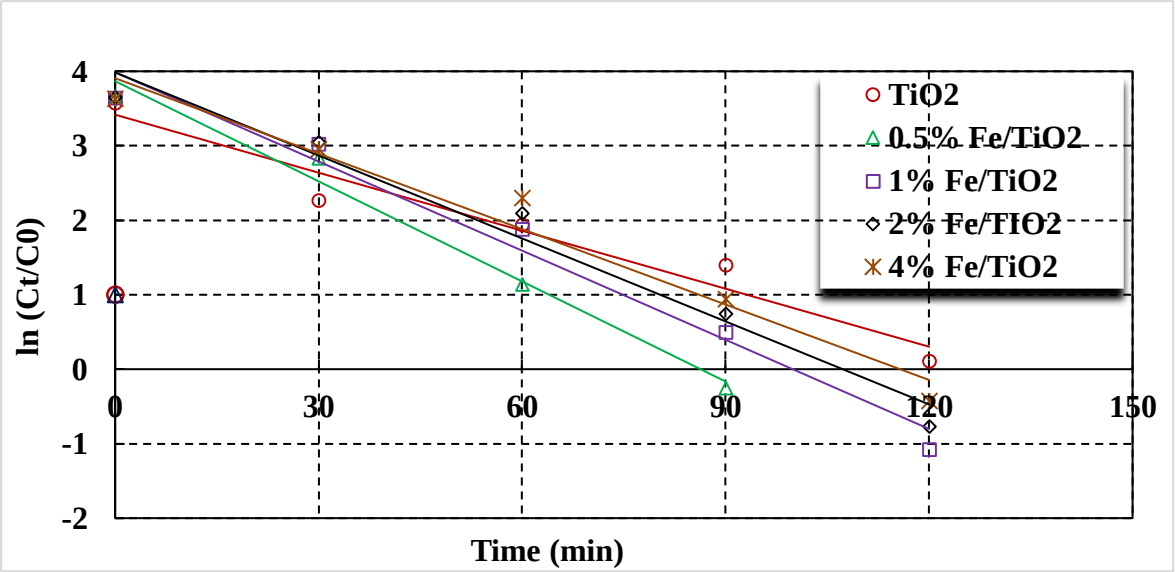

Figure 4.13: Pseudo-first order kinetics of caffeine degradation

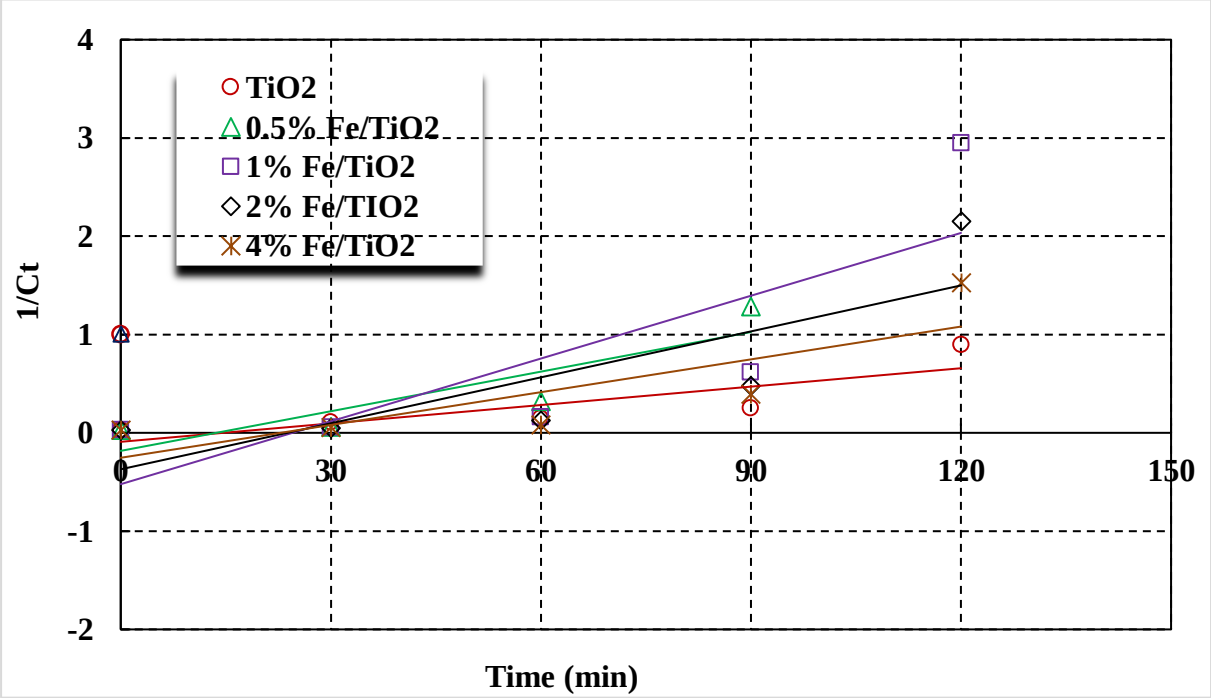

Figure 4.14: Pseudo-second order kinetics of caffeine degradation

The reaction rate coefficients for first order (k_1) and second order (k_2) were calculated and presented in *Table 4.3* and *Table 4.4.*

Table 4.3: Reaction rate coefficients of pseudo-first order kinetics for caffeine photocatalytic degradation

Sample	k_1(L*mol^{-1}*min^{-1})	R^2
TiO_2	0.026	0.951
0.5 % Fe/TiO_2	0.044	0.984
1 % Fe/TiO_2	0.039	0.976
2 % Fe/TiO_2	0.037	0.972
4 % Fe/TiO_2	0.033	0.939

Table 4.4: Reaction rate coefficients of pseudo-second order kinetics for caffeine photocatalytic degradation

Sample	k_2 (L*mol^{-1}*min^{-1})	R^2
TiO_2	0.0062	0.715
0.5 % Fe/TiO_2	0.0134	0.783
1 % Fe/TiO_2	0.0213	0.659
2 % Fe/TiO_2	0.0156	0.667
4 % Fe/TiO_2	0.0112	0.682

From *Table 4.3* it can be seen that the experimental data were best fitted by the pseudo-first-order model.

The assessment of energy consumption of the ultraviolet lamp is crucial because it has an impact on the operating cost of wastewater technology. For pseudo-order kinetics, the electric energy per order E_{EO} (kWh/m^3/order) can be defined by using the following *Equation 4.20*. The equation is applied for the batch reactor [83].

$$E_{EO}=\frac{P*t*1000}{V*60*log(\frac{C_0}{C_f})} \quad (4.20)$$

P=electric power of the UV lamp, kW

t = irradiation time, min

V=the volume of treated wastewater, L

C_0 = the initial concentration of the pollutant, mg L^{-1}

C_f = the final concentration of the pollutant, mg L^{-1}

TC values were used for C_0 and C_f and the obtained results are depicted in *Table 4.4*.

Table 4.5: The consumption of electrical energy per treatment process

Sample	E_{EO} kWh/m^3/order
UV + TiO_2	17602
UV+0.5 % Fe/TiO_2	17045
UV + 1 % Fe/TiO_2	19517
UV + 2 % Fe/TiO_2	19434
UV + 4 % Fe/TiO_2	18470

The obtained results showed a high value of consumption of electrical energy for treatment processes. Singh et al. [84] noted that the addition of oxidative agents can significantly reduce the consumption of electrical energy.

Chapter 5 - Conclusion

Caffeine was used as an emerging pollutant for all experiments including Ag modified catalysts and Fe-doped TiO_2 catalysts. The obtained results by using Ag modified zeolites did not meet the expectations. It is important to note that zeolite was applied in the performed experiments is of natural type. As the porosity of natural zeolites has a great impact on the experiment results, for natural zeolites it is hard to obtain uniform porous structure.

From the study, it can be seen that caffeine removal can be achieved by TiO_2 (Aeroxide 25) using ultraviolet light 365 nm. However, Bouanimba et al. [77] reported that photodegradation of caffeine using TiO_2 (rutile phase) is negligible (10%). The big difference was obtained in the results of TC and HPLC values. That was explained since caffeine has various intermediates which are more stable in aqueous solution. The photocatalytic degradation of caffeine was successfully achieved with all Fe-doped TiO_2 catalysts. The TC removal of caffeine with UV/Fe-doped TiO_2 was similar to UV/TiO_2. All photocatalysts achieved 100% caffeine removal. This also illustrates the difference between the HPLC and TC results.

The HPLC apparatus could not able to identify the specific by-products of caffeine. Thus, for this purpose other equipment should be applied, for example, GCMS (Gas chromatography-mass spectroscopy) and IC analysis to check for possible intermediates.

In this work, catalytic and photocatalytic processes were implemented for the treatment of caffeine solution. Ag modified zeolites and Fe-doped TiO_2 catalysts were synthesized their catalytic/photocatalytic efficiency was examined. The main conclusions are:

a) The study illustrates low- technology and simple method of Ukrainian clinoptilolite modification with $AgNO_3$. A following physical-chemical process of zeolites causes the silver species formation. The successful doping of Ag particle to the zeolite was affirmed by XRD, XRF, SEM and TEM analysis.
b) XRD analysis results confirm the formation of Ag particles by diffraction peaks of Ag, Ag_2O and Ag particles.
c) XRF analysis results showed that Ag^0_NZU possesses the highest amount of Ag particles (2.38%).

d) From SEM results it is seen that c_Ag^+_NZU catalyst has a more uniform structure than other modified zeolites. TEM results show that *Ag^+_NZU* has the biggest size of particles, however other modified zeolites have the size between 8 to 30 nm.
e) UV light 254 nm have negligible removal of caffeine from aqueous solution. Thus it is not recommended.
f) The combination of Ag modified zeolites with UV light 254 nm did not improve the performance of the caffeine removal. However, the caffeine removal by using UV light was 4% and it was increased to 20% using *Ag^0_NZU* catalyst.
g) The treatment of caffeine solution was studied by UV/TiO_2 (Degussa 25). It is observed from HPLC analysis that caffeine removal had 100% and TC removal increased slowly.
h) Fe-doped TiO_2 catalysts with different iron concentrations (0.5%, 1%, 2%, 4%) were examined for treatment of caffeine solution under ultraviolet light 365 nm. The mineralization of caffeine solution was successfully done by using all catalysts. The caffeine removal by HPLC analysis was higher than TC removal. It was explained by the formation of caffeine intermediates.
i) Using experimental data a pseudo-first-order kinetic model was obtained for degradation of caffeine reaction. The reaction rate constant and energy consumption was obtained.

Future work will include a study of various catalytic/photocatalytic processes for the treatment of various emerging pollutants. For enhancing the treatment of caffeine solution oxidizing agents can be used. Also, dopant Ag can be changed with other doping materials. Also, the other natural or synthetic zeolites can be tested. In the case of Fe-doped TiO_2 catalysts, other emerging pollutants could be examined. Also, catalyst doping material can be changed to other materials.

Bibliography/References

[1] **Kumar, P., *et al.,*** "Hydrothermal synthesis of Cu-ZnO-/TiO 2-based engineered nanomaterials for the efficient removal of organic pollutants and bacteria from water," BioNanoScience, 7(4), pp. 574-582, (2017).

[2] **Rodriguez-Narvaez, O.M., *et al.,*** "Treatment technologies for emerging contaminants in water: a review," *Chemical Engineering Journal*, 323, pp. 361-380, (2017).

[3] **Teodosiu, C., *et al..,*** "Emerging pollutants removal through advanced drinking water treatment: a review on processes and environmental performances assessment," Journal of Cleaner Production, 197, pp. 1210-1221, (2018).

[4] **Rodil, R., *et al..,*** "Multi-residue analytical method for the determination of emerging pollutants in water by solid-phase extraction and liquid chromatography–tandem mass spectrometry," Journal of Chromatography A, 1216 (14) pp. 2958-2969, (2009).

[5] **Houtman, C. J.,**"Emerging contaminants in surface waters and their relevance for the production of drinking water in Europe," Journal of Integrative Environmental Sciences, 7 (4), pp. 271-295, (2010).

[6] **Geissen, V.,** "Emerging pollutants in the environment: a challenge for water resource management," International soil and water conservation research, 3 (1), pp. 57-65, (2015).

[7] **Rodil, R., *et al..,*** "Legacy and emerging pollutants in marine bivalves from the Galician coast (NW Spain)," Environment international, 129, pp. 364-375, (2019).

[8] **Guillén, D.,** "Prioritization of chemicals in the aquatic environment based on risk assessment: analytical, modeling and regulatory perspective," Science of the Total Environment, 440, pp. 236-252, (2012).

[9] **Fawell, J., and C. N. Ong,** "Emerging contaminants and the implications for drinking water," International Journal of Water Resources Development, 28 (2), pp. 247-263 (2012).

[10] **Krishnan, S.,** "Comparison of various advanced oxidation processes used in remediation of industrial wastewater laden with recalcitrant pollutants," Materials Science and Engineering, 206 (1) p.012089 (Jun.2017)

[11] **Bhargava, A.,** "Physico-chemical waste water treatment technologies: an overview," Int J Sci Res Educ, 4 (5), pp. 5308-5319 (2016).

[12] **Sonune, A., and R. Ghate,** "Developments in wastewater treatment methods," Desalination, 167, pp. 55-63 (2004).

[13] **Gerba, C. P., and I. L. Pepper,** "Municipal Wastewater Treatment," Environmental and Pollution Science, pp. 393-418. (2019).

[14] **Kraslawski, A., and I. Turunen**, 23rd European Symposium on Computer Aided Process Engineering: Elsevier, (2013).

[15] **Wang, J. L., and L. J. Xu,** "Advanced oxidation processes for wastewater treatment: formation of hydroxyl radical and application," Critical reviews in environmental science and technology, 42 (3), pp. 251-325 (2012).

[16] **Deng, Y., and R. Zhao,** "Advanced oxidation processes (AOPs) in wastewater treatment," Current Pollution Reports, 1 (3), pp. 167-176 (2015).

[17] **Sharma, S., *et al.,*** "A general review on advanced oxidation processes for waste water treatment," Institute of Technology, Nirma University, Ahmedabad-382, 481, pp. 08-10 (2011).

[18] **Munter, R.,**"Advanced oxidation processes–current status and prospects," Proc. Estonian Acad. Sci. Chem, 50 (2) pp. 59-80 (2001).

[19] **Mishra, M., and S. K. Jain,** "Properties and applications of zeolites: A Review," Proceedings of the National Academy of Sciences India Section B-Biological Sciences, 81, pp. 250-259 (2011).

[20] **Jha, B.,** "DNS, Fly Ash Zeolites: Innovations, Applications, and Directions," Springer, (2016).

[21] **Wang, S., and Y. Peng,** "Natural zeolites as effective adsorbents in water and wastewater treatment," Chemical Engineering Journal, 156 (1), pp. 11-24 (2010).

[22] **Mgbemere, H., *et al.,*** "Zeolite synthesis, characterization and application areas: a review," Int Res J Environ Sci, 6 (10), pp. 45-49 (2017).

[23] **Adam, M. R., *et al*** "Feasibility study of the hybrid adsorptive hollow fibre ceramic membrane (HFCM) derived from natural zeolite for the removal of ammonia in wastewater," Process Safety and Environmental Protection, 122, pp. 378-385 (2019).

[24] **Nezamzadeh-Ejhieh, A., and S. Moeinirad,** "Heterogeneous photocatalytic degradation of furfural using NiS-clinoptilolite zeolite," Desalination, 273 (2-3), pp. 248-257 (2011).

[25] **Nikazar, M., *et al.,*** "Photocatalytic degradation of azo dye Acid Red 114 in water with TiO2 supported on clinoptilolite as a catalyst," Desalination, 219 (1-3), pp. 293-300 (2008).

[26] **Wardhani, S., *et al.,*** "Photocatalytic Degradation of Methylene Blue Using TiO_2-Natural Zeolite as A Photocatalyst," The Journal of Pure and Applied Chemistry Research, 5(1), pp. 19-27 (2016).

[27] **Liu, S., *et al.,*** "TiO_2-coated natural zeolite: rapid humic acid adsorption and effective photocatalytic regeneration," Chemical Engineering Science, 105, pp. 46-52 (2014).

[28] **Abidin, A., *et al.,*** "Rapid degradation of methyl orange by Ag doped zeolite X in the presence of borohydride," *Journal of Taibah University for Science, 11*(6), 1070-1079 (2017).

[29] **Huang, M., *et al.,*** "Photocatalytic discolorization of methyl orange solution by Pt modified TiO_2 loaded on natural zeolite" Dyes and pigments, 77 (2), pp. 327-334 (2008).

[30] **Liu, X. H., *et al.,*** "Characterization on the microstructures and optical performances of TiO_2 doped with transition metals," pp. 388-394 (2014).

[31] **Castañeda-Juárez, M., *et al.,*** "Synthesis of TiO_2 catalysts doped with Cu, Fe, and Fe/Cu supported on clinoptilolite zeolite by an electrochemical-thermal method for the degradation of diclofenac by heterogeneous photocatalysis," Journal of Photochemistry and Photobiology A: Chemistry, 380, pp. 111834 (2019).

[32] **Mirzaei, N., *et al.,*** "Modified natural zeolite using ammonium quaternary based material for Acid red 18 removal from aqueous solution," Journal of environmental chemical engineering, 5 (4), pp. 3151-3160 (2017).

[33] **Taffarel, S. R., and J. Rubio,** "Adsorption of sodium dodecyl benzene sulfonate from aqueous solution using a modified natural zeolite with CTAB," Minerals Engineering, vol. 23 (10), pp. 771-779, (2010).

[34] **Georgiev, D *et al.,*** "Synthetic zeolites–Structure, classification, current trends in zeolite synthesis," In Economics and Society Development on the Base of Knowledge: International Scientific Conference, 7, (2009).

[35] **Durgakumari, V., *et al.,*** "An easy and efficient use of TiO_2 supported HZSM-5 and TiO_2+ HZSM-5 zeolite combinate in the photodegradation of aqueous phenol and p-chlorophenol," Applied Catalysis A: General, 234 (1-2), pp. 155-165 (2002).

[36] **Zhao, C., *et al.,*** "Photodegradation of oxytetracycline in aqueous by 5A and 13X loaded with TiO2 under UV irradiation," Journal of hazardous materials, 176, (1-3), pp. 884-892 (2010).

[37] **Pan, Z., *et al.,*** "Photocatalytic degradation of 17α-ethinylestradiol (EE2) in the presence of TiO2-doped zeolite," Journal of hazardous materials, 279, pp. 17-25 (2014).

[38] **Zhang, W., *et al.,*** "Fabrication of TiO2/MoS2@ zeolite photocatalyst and its photocatalytic activity for degradation of methyl orange under visible light," Applied Surface Science, 358, pp. 468-478 (2015).

[39] **Zhang, G., *et al.,*** "Selective photocatalytic degradation of aquatic pollutants by titania encapsulated into FAU-type zeolites," Journal of hazardous materials, 188 (1-3), pp. 198-205 (2011).

[40] **Hashemi, A., *et al.,*** "Organic contaminants removal from industrial wastewater by CTAB treated synthetic zeolite," Y. Journal of environmental management, 233, pp. 785-792 (2019).

[41] **Gjyli, S., *et al.,*** "Higher conversion rate of phenol alkylation with diethylcarbonate by using synthetic fly ash-based zeolites," Microporous and Mesoporous Materials, 284, pp. 434-442 (2019).

[42] **Ren, X., *et al.,*** "Synthesis and characterization of single-phase submicron zeolite Y from coal fly ash and its potential application for acetone adsorption," Microporous and Mesoporous Materials, 295, pp. 109940 (2020)

[43] **Andreozzi, R *et al.,*** "Advanced oxidation processes (AOP) for water purification and recovery," Catalysis today, 53 (1), pp. 51-59 (1999)

[44] **Kuo, W.,** "Decolorizing dye wastewater with Fenton's reagent," Water Research, 26 (7), pp. 881-886 (1992).

[45] **Oturan, M. A., and J.J. Aaron,** "Advanced oxidation processes in water/wastewater treatment: principles and applications. A review," Critical Reviews in Environmental Science and Technology, 44 (23) pp. 2577-2641 (2014).

[46] **Bautista, P., *et al.,*** "An overview of the application of Fenton oxidation to industrial wastewaters treatment," Journal of Chemical Technology & Biotechnology: International Research in Process, Environmental & Clean Technology, 83 (10), pp. 1323-1338 (2008).

[47] **Chekir, N., *et al.,*** "Photocatalytic degradation of methylene blue in aqueous suspensions using TiO_2 and ZnO," Desalination and Water Treatment, 57(13), pp. 6141-6147 (2016).

[48] **Ahmad, R., *et al.,*** "Photocatalytic systems as an advanced environmental remediation: Recent developments, limitations and new avenues for applications," Journal of Environmental Chemical Engineering, 4 (4), pp. 4143-4164 (2016).

[49] **Laoufi, N., *et al.,*** "The degradation of phenol in water solution by TiO_2 photocatalysis in a helical reactor," Global NEST Journal, 10 (3), pp. 404-418 (2008).

[50] **Stasinakis, A.,** "Use of selected advanced oxidation processes (AOPs) for wastewater treatment–a mini review," Global NEST journal, 10 (3), pp. 376-385, (2008).

[51] **Choi, W., *et al.,*** "The role of metal ion dopants in quantum-sized TiO2: correlation between photoreactivity and charge carrier recombination dynamics," The Journal of Physical Chemistry, 98 (51), pp. 13669-13679 (2002).

[52] **Vargas, X. M., *et al.,*** "Characterization and Photocatalytic Evaluation (UV-Visible) of Fe-doped TiO_2 Systems Calcined at Different Temperatures," Journal of Advanced Oxidation Technologies, 18 (1), pp. 129-138 (2015).

[53] **Trovó, A,G., *et al.,*** "Degradation of caffeine by photo-Fenton process: Optimization of treatment conditions using experimental design," Chemosphere, 90 (2), pp. 170-175 (2013).

[54] **Siciliano, A.,** "TiO_2 photocatalytic degradation of caffeine and exotoxicological assessment of oxidation by products" (2014).

[55] **Sodré, F, F., *et al.*, "**Occurrence of emerging contaminants in Brazilian drinking waters: a sewage-to-tap issue," *Water, Air, and Soil Pollution,* 206 (1-4), pp. 57-67 (2010).

[56] **Sharma, B. M., *et al.*,** "Health and ecological risk assessment of emerging contaminants (pharmaceuticals, personal care products, and artificial sweeteners) in surface and groundwater (drinking water) in the Ganges River Basin, India," Science of the Total Environment, 646, pp. 1459-1467 (2019).

[57] **Manamsa, K., *et al.*,** "A national-scale assessment of micro-organic contaminants in groundwater of England and Wales," Science of the Total Environment, 568, pp. 712-726 (2016).

[58] **Moore, M., *et al.*,** "Assessing caffeine as an emerging environmental concern using conventional approaches," Archives of environmental contamination and toxicology, 54 (1), pp. 31-35 (2008).

[59] **Busse, L., and C. Nagoda,** "Detection of Caffeine in the Streams and Rivers within the San Diego Region–Pilot Study," SWAMP–Surface Water Ambient Monitoring Program, California Regional Water Quality Control Board, San Diego Region, (2015).

[60] **Gokulakrishnan, S.,** "Microbial and enzymatic methods for the removal of caffeine," Enzyme and Microbial Technology, 37 (2), pp. 225-232 (2005).

[61] **Elhalil, A.,** "Photocatalytic degradation of caffeine as a model pharmaceutical pollutant on Mg doped ZnO-Al2O3 heterostructure," Environmental nanotechnology, monitoring & management, 10, pp. 63-72 (2018).

[62] **Sacco, O., *et al.*,** "ZnO supported on zeolite pellets as efficient catalytic system for the removal of caffeine by adsorption and photocatalysis," Separation and Purification Technology, 193, pp. 303-310 (2018).

[63] Agilent InfinityLab LC Series. 1290 Infinity II High Speed Pump. User Manual (2016).

[64] Agilent InifinityLab LC Series. Multisamplers. User Manual (2017).

[65] Agilent InfinityLab LCSeries. 1290 II Multicolumn Thermostat. User Manual (2016).

[66] Analytic Jena AG, "TOC/TNb Analysis in Water and Liquid Samples".

[67] **Chen, Y. C., and K.P. Yu,** "Enhanced antimicrobial efficacy of thermal-reduced silver nanoparticles supported by titanium dioxide," Colloids and Surfaces B: Biointerfaces, 154, pp. 195-202 (2017).

[68] **Hernández-Alonso, M.D., *et al.*,** "Development of alternative photocatalysts to TiO_2: challenges and opportunities," Energy & Environmental Science, 2 (2), pp. 1231-1257 (2009).

[69] **Hakil, M., *et al.*, "**Degradation and product analysis of caffeine and related dimethylxanthines by filamentous fungi," Enzyme and Microbial Technology, 22 (5), pp. 355-359 (1998).

[70] **Tauanov, Z.,and V. Inglezakis,** "Removal of iodide from water using silver nanoparticles-impregnated synthetic zeolites," Science of The Total Environment, 682, pp. 259-270 (2019).

[71] **Liu, S., et al.,** "TiO_2-coated natural zeolite: rapid humic acid adsorption and effective photocatalytic regeneration", Chemical Engineering Science, 105, pp. 46-52 (2014).

[72] **Korobeinyk, A., *et al.*,** "Iodide Removal by Use of Ag-Modified Natural Zeolites." 182(1), p. 012014 (2018).

[73] **Onkani, S.P. *et al.*,**"Comparative study of the photocatalytic degradation of 2–chlorophenol under UV irradiation using pristine and Ag-doped species of TiO_2, ZnO and ZnS photocatalysts," Journal of Environmental Management, 260, pp. 110145 (2020).

[74] **Vaiano, V. *et al.*,** "UV and visible-light driven photocatalytic removal of caffeine

using ZnO modified with different noble metals (Pt, Ag and Au),” Materials Research Bulletin, vol. 112, pp. 251-260 (2019).

[75] **Crittenden, J. C. *et al.,*** MWH's water treatment: principles and design: John Wiley & Sons, (2012).

[76] **Mezioud, N., *et al.,*** “Methabenzthiazuron degradation with illuminated TiO_2 aqueous suspensions. Kinetic and reactional pathway investigations,” Journal of Photochemistry and Photobiology A: Chemistry, 288, pp. 13-22 (2014).

[77] **Bouanimba, N., *et al.,*** “A Comparative Study of the Activity of TiO_2 Degussa P25 and Millennium PCs in the Photocatalytic Degradation of Bromothymol Blue,” International Journal of Chemical Reactor Engineering, 16 (4), (2017).

[78] **Yu, J., *et al.,*** “Preparation, characterization and visible-light-driven photocatalytic activity of Fe-doped titania nanorods and first-principles study for electronic structures,” Applied Catalysis B: Environmental, 90 (3-4), pp. 595-602 (2009).

[79] **Vargas, X. M., *et al.,*** “Characterization and Photocatalytic Evaluation (UV-Visible) of Fe-doped TiO_2 Systems Calcined at Different Temperatures,” Journal of Advanced Oxidation Technologies, 18 (1), pp. 129-138 (2015).

[80] **Zhu, J., *et al.,*** “Fe^{3+} TiO_2photocatalysts prepared by combining sol–gel method with hydrothermal treatment and their characterization,” Journal of Photochemistry and Photobiology A: Chemistry, 180 (1-2), pp. 196-204 (2006).

[81] **Matafonova, G., *et al.,*** “Degradation of chlorophenols in aqueous media using UV XeBr excilamp in a flow-through reactor,” Chemosphere, 70 (6), pp. 1124-1127 (2008).

[82] **Andreozzi, R., *et al.,*** “Photocatalytic oxidation of 4-nitrophenol in aqueous TiO_2 slurries: an experimental validation of literature kinetic models,” Journal of Chemical Technology & Biotechnology: International Research in Process, Environmental & Clean Technology, 75 (2), pp. 131-136 (2000).

[83] **Asaithambi, P., *et al.,* “**Electrical energy per order determination for the removal pollutant from industrial wastewater using UV/Fe^{2+} /H_2O_2 process: optimization by response surface methodology,” Water Resources and Industry, 18, pp. 17-32 (2017).

[84] **Singh, P. *et al.,*** “Energy pattern analysis of a wastewater treatment plant,” Applied Water Science, 2 (3), pp. 221-226 (2012).

Appendix A

XRF analysis of silver modified zeolites

Compound	Value	Unit	Status
Na2O	1,238	%	BgC;DC;
MgO	0,196	%	BgC;DC;
Al2O3	11,527	%	BgC;DC;
SiO2	77,253	%	BgC;DC;
SO3	0,056	%	BgC;DC;
K2O	2,197	%	BgC;DC;
CaO	0,721	%	BgC;DC;
TiO2	0,167	%	BgC;DC;
MnO	0,031	%	BgC;DC;
Fe2O3	1,496	%	BgC;DC;
NiO	0,021	%	BgC;DC;
Br	2,538	%	BgC;DC;
SrO	0,035	%	BgC;DC;
Y2O3	0,014	%	BgC;DC;
ZrO2	0,017	%	BgC;DC;
Ag2O	2,340	%	BgC;DC;
CeO2	0,110	%	BgC;DC;
PtO2	0,020	%	BgC;DC;

Figure A.1:Chemical composition of *Ag^{+}_NZU*

Compound	Value	Unit	Status
Na2O	1,086	%	BgC;DC;LoR;
MgO	0,230	%	BgC;DC;
Al2O3	11,333	%	BgC;DC;LoR;
SiO2	77,675	%	BgC;DC;
SO3	0,045	%	BgC;DC;
K2O	2,249	%	BgC;DC;
CaO	0,711	%	BgC;DC;
TiO2	0,156	%	BgC;DC;
Fe2O3	1,511	%	BgC;DC;
ZnO	0,009	%	BgC;DC;
Br	2,328	%	BgC;DC;
SrO	0,030	%	BgC;DC;
Y2O3	0,015	%	BgC;DC;
ZrO2	0,012	%	BgC;DC;LoR;
Nb2O5	0,006	%	BgC;DC;
Ag2O	2,361	%	BgC;DC;
BaO	0,073	%	BgC;DC;
CeO2	0,118	%	BgC;DC;

Figure A.2:Chemical composition of *Ag_2O_NZU*

Compound	Value	Unit	Status
Na2O	1,351	%	BgC;DC;
MgO	0,250	%	BgC;DC;
Al2O3	11,297	%	BgC;DC;
SiO2	78,485	%	BgC;DC;
SO3	0,048	%	BgC;DC;
K2O	2,100	%	BgC;DC;
CaO	0,724	%	BgC;DC;
TiO2	0,155	%	BgC;DC;
MnO	0,040	%	BgC;DC;
Fe2O3	1,433	%	BgC;DC;
NiO	0,023	%	BgC;DC;
CuO	0,019	%	BgC;DC;
Br	2,208	%	BgC;DC;
SrO	0,034	%	BgC;DC;
ZrO2	0,012	%	BgC;DC;LoR;
Ag2O	1,758	%	BgC;DC;
PtO2	0,033	%	BgC;DC;
Au	0,029	%	BgC;DC;IC;

Figure A.3:Chemical composition of *c_Ag^{+}_NZU*

Compound	Value	Unit	Status
Na2O	1,621	%	BgC;DC;LoR;
MgO	0,210	%	BgC;DC;
Al2O3	10,994	%	BgC;DC;LoR;
SiO2	77,098	%	BgC;DC;
SO3	0,055	%	BgC;DC;
K2O	2,318	%	BgC;DC;
CaO	0,754	%	BgC;DC;
TiO2	0,195	%	BgC;DC;LoR;
MnO	0,051	%	BgC;DC;
Fe2O3	1,582	%	BgC;DC;
NiO	0,014	%	BgC;DC;
ZnO	0,008	%	BgC;DC;
Br	2,351	%	BgC;DC;
SrO	0,036	%	BgC;DC;
ZrO2	0,019	%	BgC;DC;
Nb2O5	0,009	%	BgC;DC;
Ag2O	2,565	%	BgC;DC;
BaO	0,075	%	BgC;DC;

Figure A.4:Chemical composition of *Ag^{0}_NZU*

Appendix B
EDS mapping of SEM analysis of silver modified zeolites

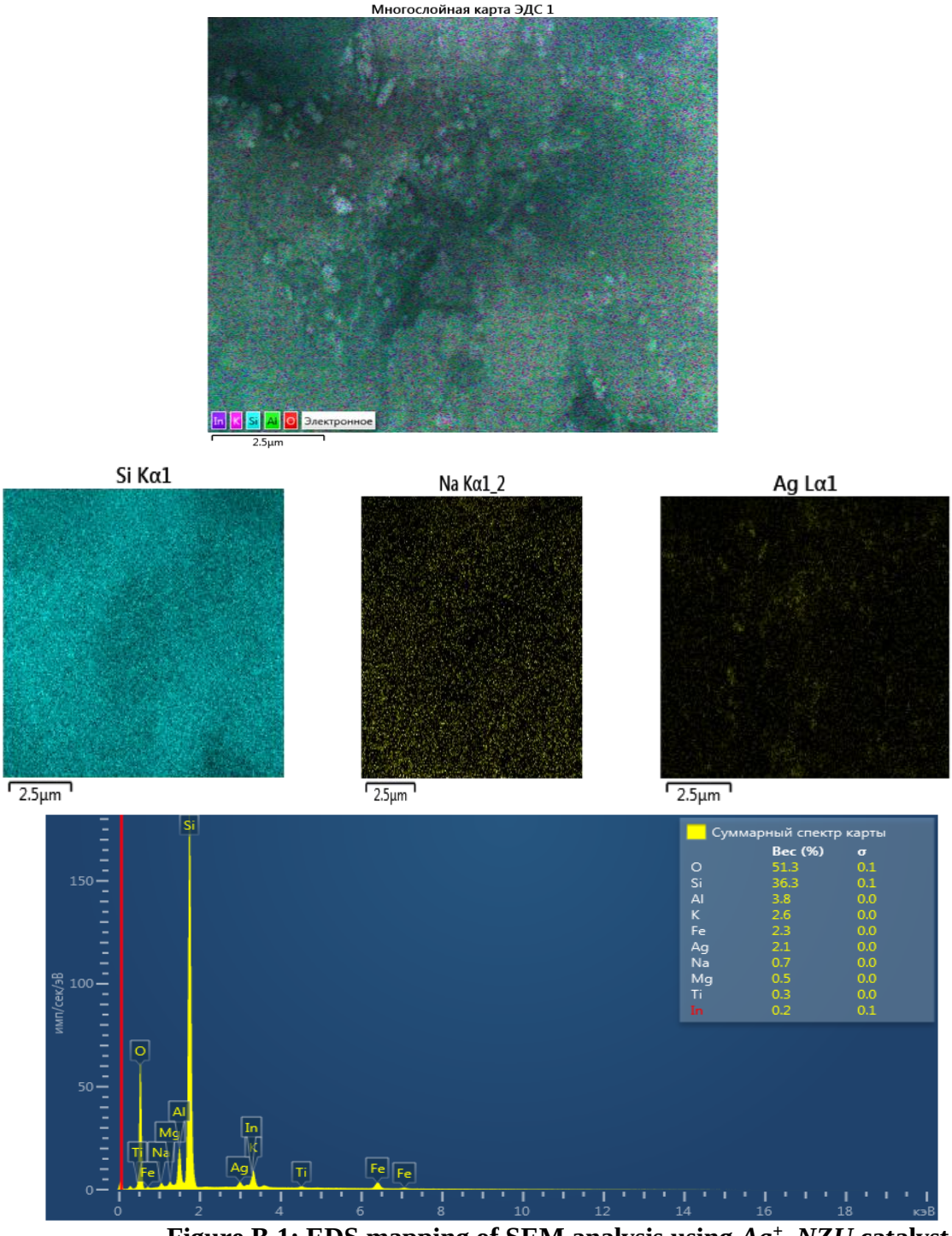

Figure B.1: EDS mapping of SEM analysis using *Ag^{+}_NZU* catalyst

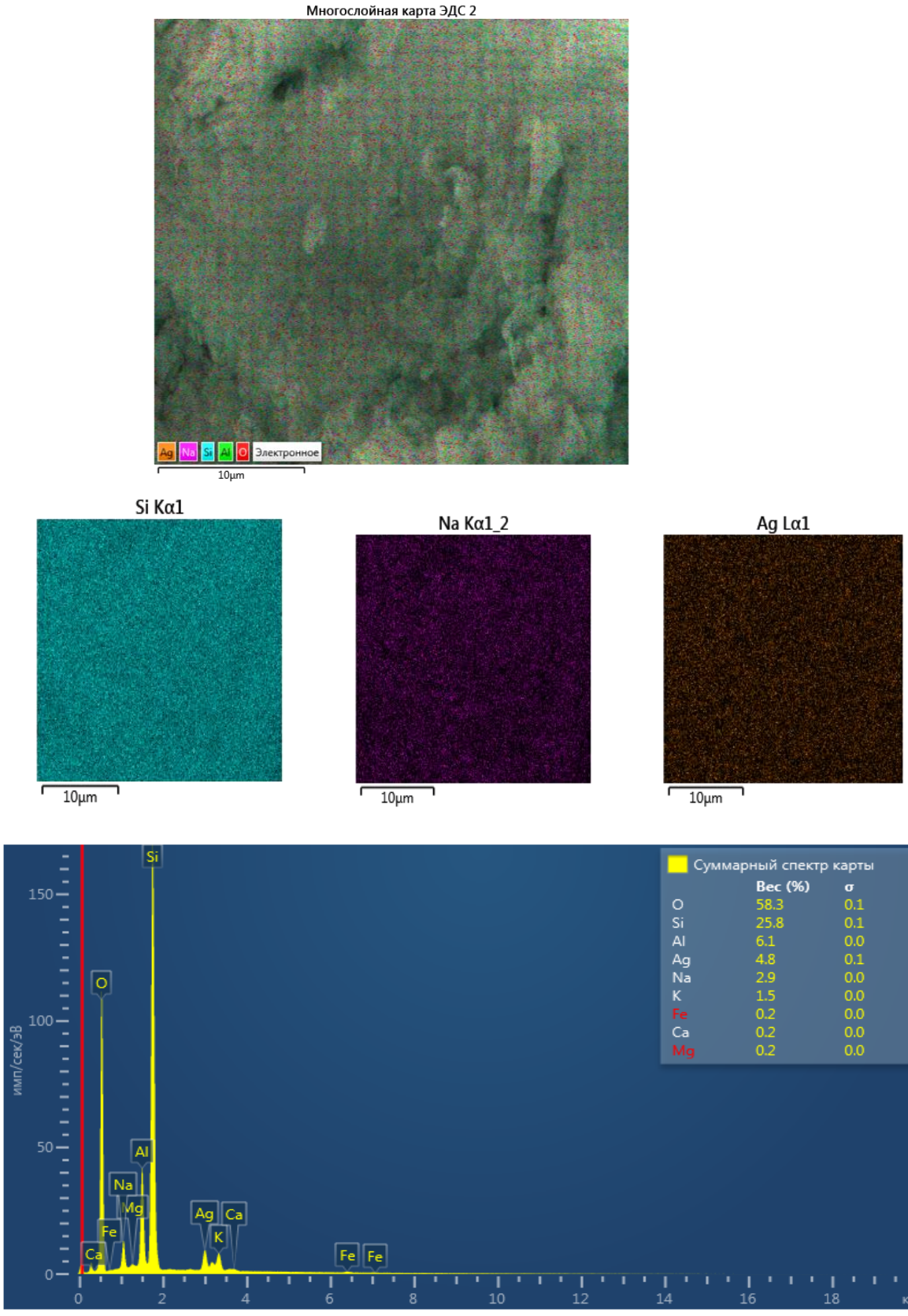

Figure B.2: EDS mapping of SEM analysis using *Ag_2O_NZU* catalyst

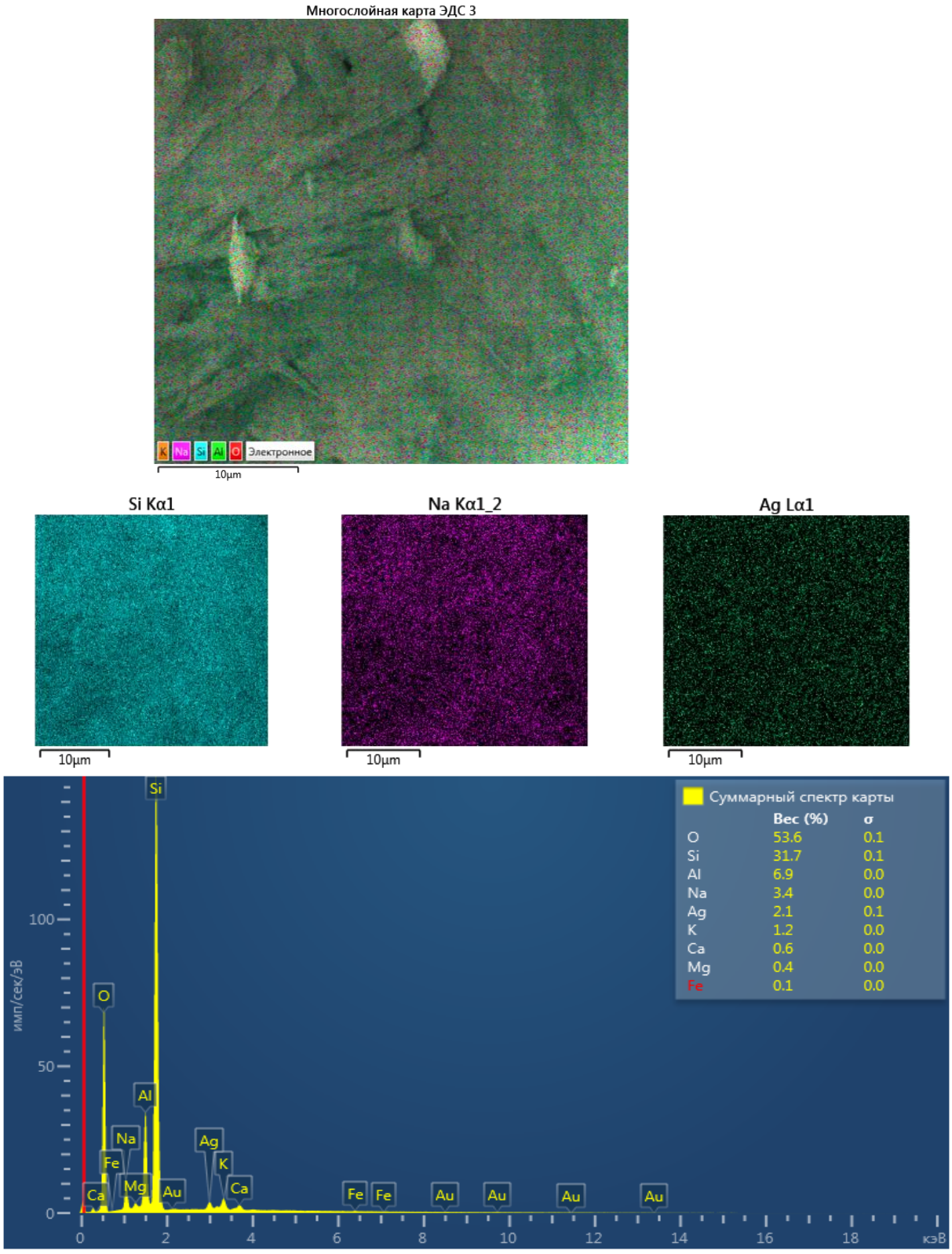

Figure B.3: EDS mapping of SEM analysis using c_*Ag*$^{+}$_*NZU* catalyst

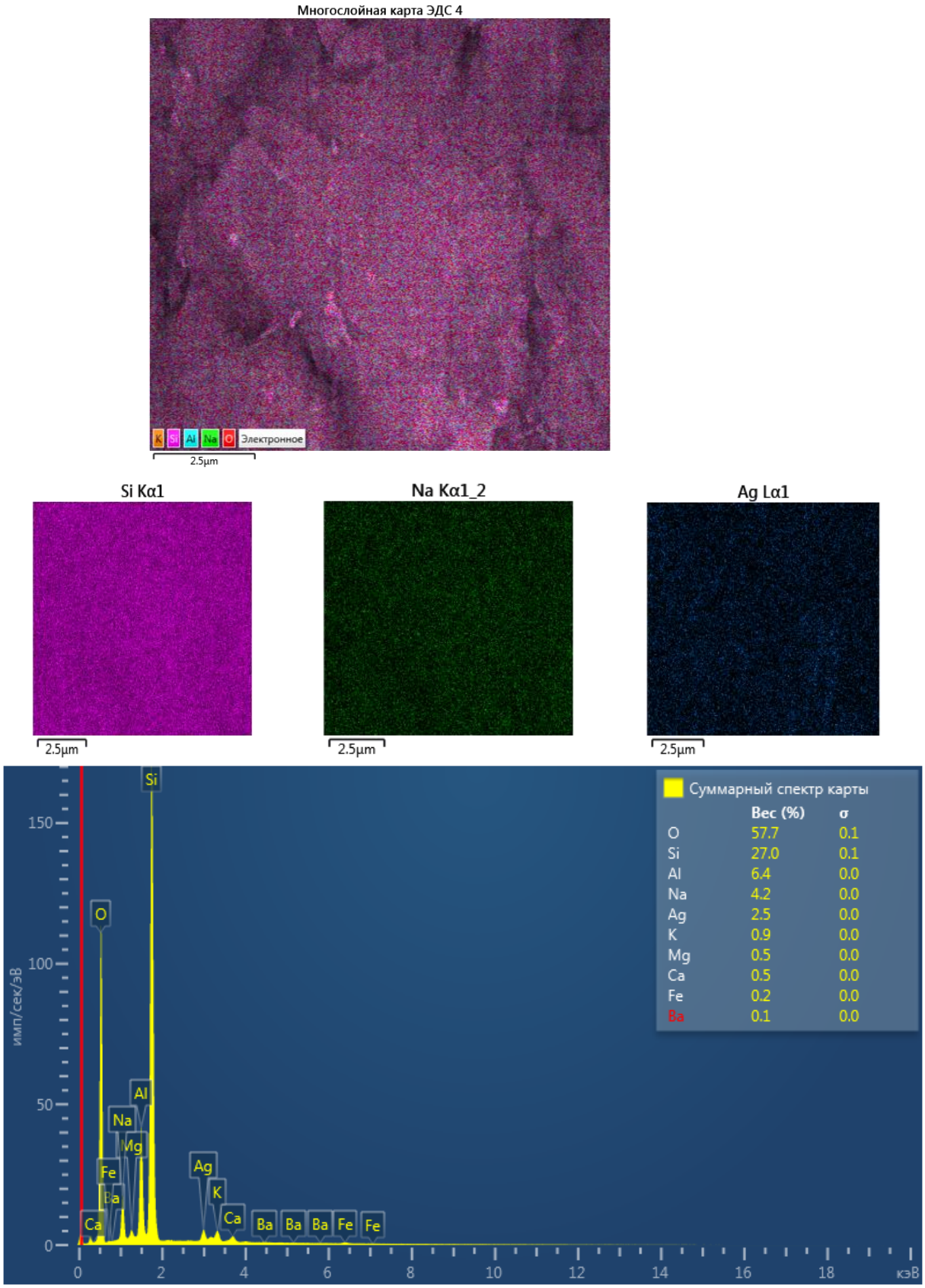

Figure B.4: EDS mapping of SEM analysis using *Ag^0_NZU* catalyst

Appendix C
SEM analysis for silver modified zeolites

Figure C.1: SEM analysis for *Ag^{+}_NZU* catalyst

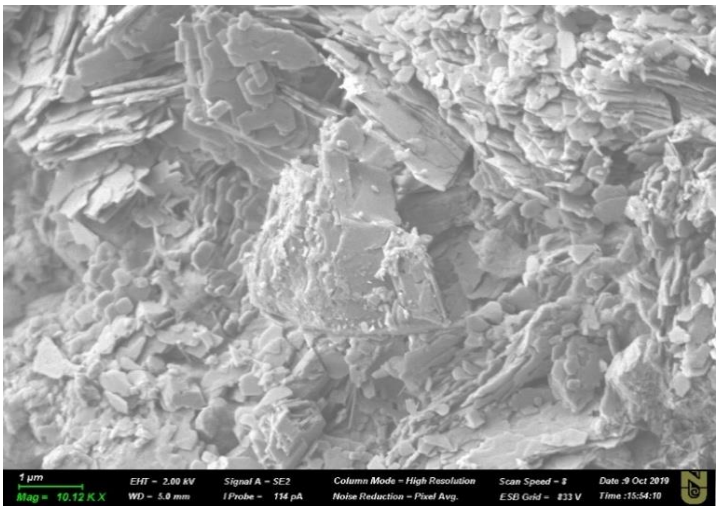

Figure C.2: SEM analysis for *Ag_2O_NZU* catalyst

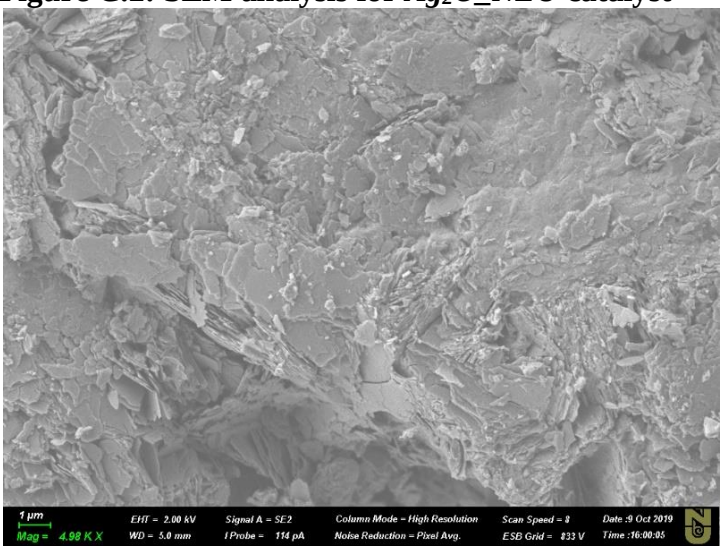

Figure C.3: SEM analysis for c*_Ag^{+}_NZU* catalyst

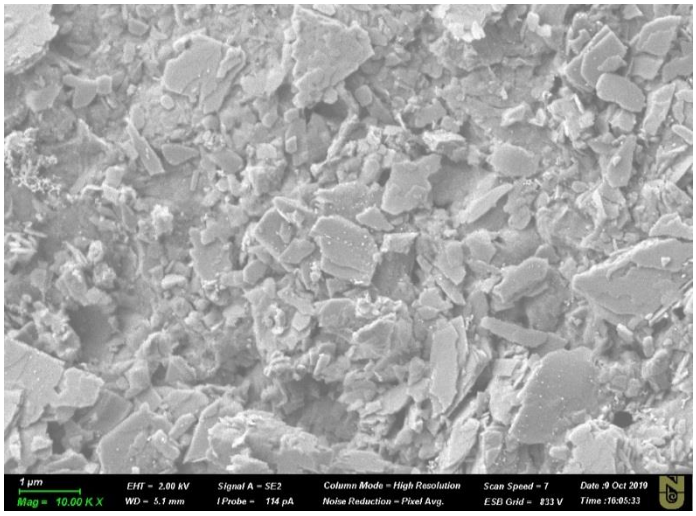

Figure C.4: SEM analysis for *Ag^0_NZU* catalyst

Appendix D
TEM analysis for all samples

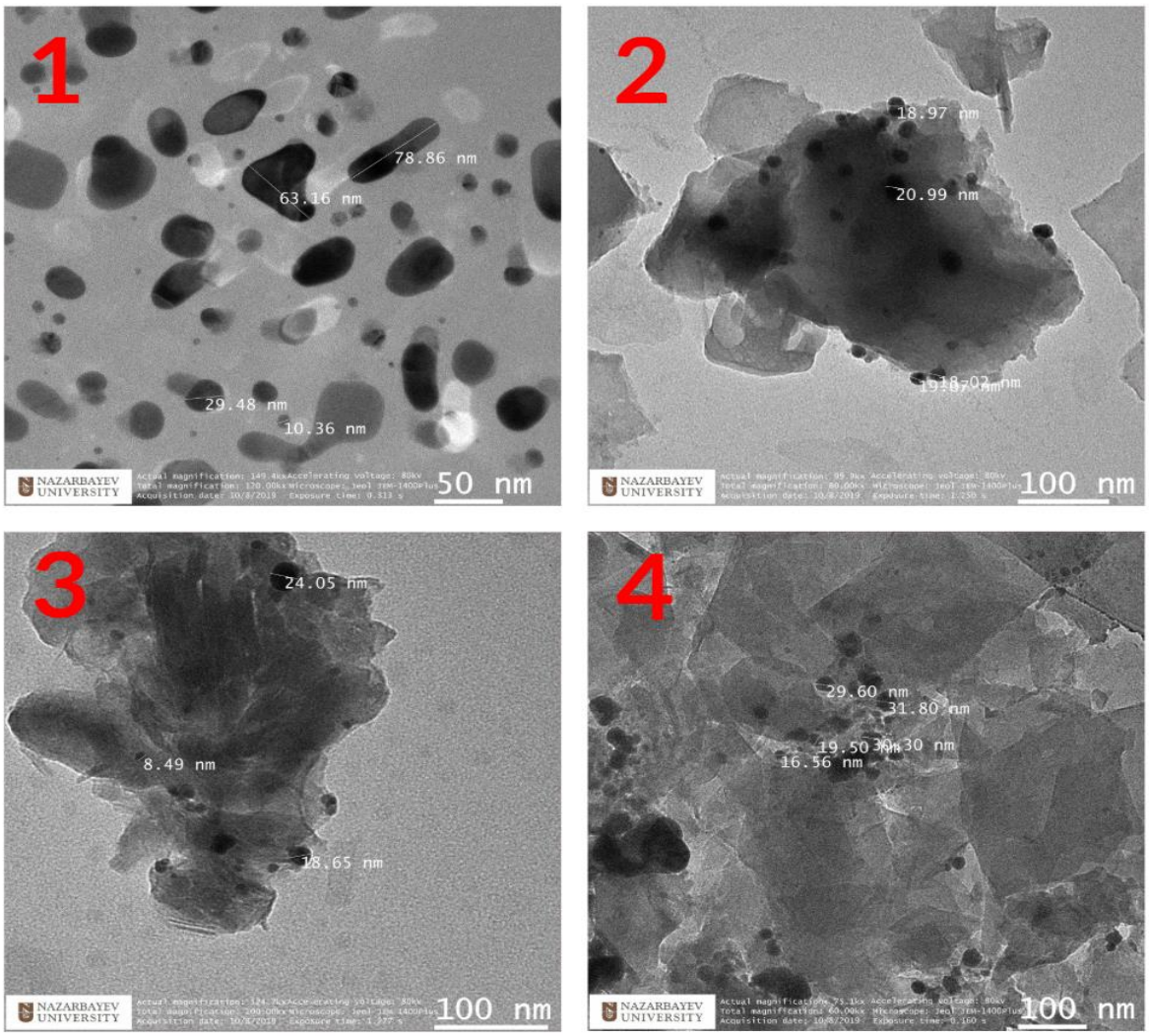

Figure D.1: TEM analysis for *silver modified catalysts. 1)Ag^+_NZU, 2)Ag_2O_NZU, 3) c_Ag^+_NZU, 4)Ag^0_NZU*